Title
Evaluating the relationships between specific drainage area characteristics and soil metal concentrations in long-established bioswales receiving suburban stormwater runoff

Authors
Feraud, Marina
Holden, Patricia A

Publication Date
2021-02-01

DOI
10.1016/j.scitotenv.2020.143778

Peer reviewed

Science of the Total Environment xxx (xxxx) xxx

Contents lists available at ScienceDirect

Science of the Total Environment

journal homepage: www.elsevier.com/locate/scitotenv

Evaluating the relationships between specific drainage area characteristics and soil metal concentrations in long-established bioswales receiving suburban stormwater runoff

Marina Feraud [a,b,*], Patricia A. Holden [a,b]

[a] Bren School of Environmental Science and Management, University of California, Santa Barbara, CA 93106, United States
[b] Earth Research Institute, University of California, Santa Barbara, CA 93106, United States

HIGHLIGHTS

- Low but quantifiable soil metals in >10-year-old suburban bioswales.
- Soil Zn concentrations correlate with impervious drainage to bioswale area ratio.
- Soil metal concentrations relate to modeled annual metal loads using regional data.
- Soil Zn and Cu total concentrations are mostly below ecological screening levels.
- Transferable field and modeling approach for informing soil bioswale management.

GRAPHICAL ABSTRACT

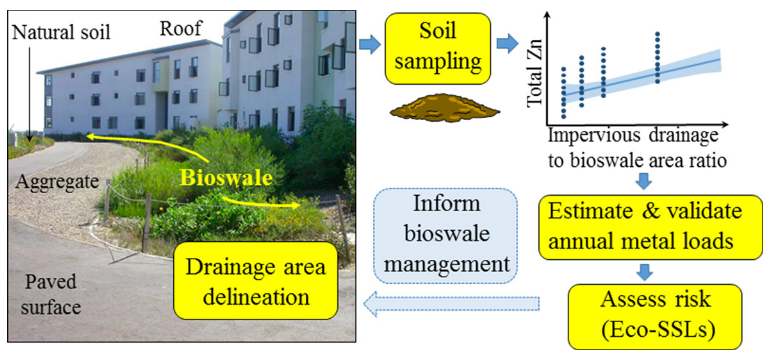

ARTICLE INFO

Article history:
Received 16 September 2020
Received in revised form 9 November 2020
Accepted 12 November 2020
Available online xxxx

Editor: Fernando A.L. Pacheco

Keywords:
Bioretention
Bioinfiltration
Impervious drainage
Metals
Ecological soil screening levels
Soil management

ABSTRACT

Bioswales are used to attenuate stormwater pollution, but their long-term sustainability regarding sequestered metals is relatively unknown, and a clear rationale for prioritizing soil management is lacking. Impervious areas draining into four 14-year-old suburban bioswales were delineated, for which surface soils (top 10 cm; 72 samples) were sampled; soils from 4 adjacent reference sites were also sampled. Total and water soluble metals (Cd, Cu, Pb, Zn) were quantified, and the relationships between metal concentrations and drainage area characteristics evaluated. Annual metal loads were estimated using regional runoff data to simulate current and future metal concentrations; risks to soil biota were assessed by comparing metal concentrations to ecological screening levels. The drainage areas' percent imperviousness (37–71%) and ratios of impervious drainage area to bioswale area (2.0–5.7) varied, owing to differing proportions of rooftops, paved surfaces, lawns, and natural soils. Total Cu and Zn ranged from 10.0 to 43.2 mg/kg dry soil, and 15.6 to 129.5 mg/kg dry soil, respectively. Across all bioswales, total Zn was positively correlated to percent impervious area ($r = 0.32$, $p = 0.0073$), the ratio of connected impervious drainage area to infiltration area ($r = 0.32$, $p = 0.0073$), and percent drainage area as paved surfaces ($r = 0.46$, $p = 5.6$ E-05), but negatively correlated to percent drainage area as lawns ($r = -0.48$; $p = 2.4$ E-05). Water soluble metal concentrations were orders of magnitude lower than total metals. Given annual metal loads (0.2–0.4 mg Cu/kg dry soil; 1.5–3.1 mg Zn/kg dry soil), replacing bioswale soils to constrain metal concentrations would be unnecessary for decades. Taken together, this study proposes a transferable approach of estimating, then verifying via sampling and analysis, bioswale soil metal concentrations, such that soil management decisions can be benchmarked to ecological screening levels.

* Corresponding author at: 2027 Bren Hall, Bren School of Environmental Science & Management, University of California, Santa Barbara, CA 93106-5131, United States.
E-mail address: mferaud@bren.ucsb.edu (M. Feraud).

https://doi.org/10.1016/j.scitotenv.2020.143778
0048-9697/

Please cite this article as: M. Feraud and P.A. Holden, Evaluating the relationships between specific drainage area characteristics and soil metal concentra..., Science of the Total Environment, https://doi.org/10.1016/j.scitotenv.2020.143778

1. Introduction

Urbanization creates and extends impervious areas by replacing natural vegetation with paved roads, roofs, parking lots and other hard surfaces that reduce infiltration and groundwater recharge, and increase stormwater runoff (Miller et al., 2014). As runoff flows overland, it incorporates pollutants deposited during dry weather, including sediments, nutrients, and metals, which can deteriorate surface water quality (NRC, 2009). To mitigate stormwater pollution, "green" and sustainable stormwater infrastructure approaches, such as bioinfiltration using biofilters and bioswales, are increasingly implemented (Jones and Davis, 2013). Bioinfiltration systems consist of excavated basins, which may or may not be vegetated, and are filled with native soil or a specified filter media (sand, compost, mulch), that sometimes is augmented with amendments such as biochar to enhance pollutant removal (Mohanty et al., 2018; Boehm et al., 2020). Pollutants in bioinfiltration systems are removed using physical, chemical and biological processes to capture, infiltrate and remediate polluted stormwater runoff (Ahiablame et al., 2012; Ambrose and Winfrey, 2015). However, there is some concern regarding the function of bioinfiltration approaches, including the fates of stormwater-derived pollutants, such as heavy metals (Li and Davis, 2008; Jones and Davis, 2013; Tedoldi et al., 2016).

Heavy metals are of concern because they persist in the environment (Giller et al., 2009) and are effectively retained in bioinfiltration soils in lab studies (e.g. Davis et al., 2003; Blecken et al., 2009; Lim et al., 2015) and at field scales (e.g. Li and Davis, 2008; Hatt et al., 2009). Metals are largely captured near stormwater runoff inlets, so that soil metal concentrations rapidly decrease in the direction of water flow (e.g. Jones and Davis, 2013; Tedoldi et al., 2017). Metal concentrations are also typically higher in the top soil layers (e.g. Sun and Davis, 2007; Hatt et al., 2008; Jones and Davis, 2013), sometimes reaching levels that are harmful to human health and soil biota (Sun and Davis, 2007; Li and Davis, 2008); as such, metals generally degrade soil quality (Li and Davis, 2008).

To address metal accumulation and soil quality concerns, to date, studies have characterized short-term metal accumulation in bioinfiltration systems and compared it to soil quality guidelines (e.g. Achleitner et al., 2007; Li and Davis, 2008); evaluated factors that influence metal loading to bioinfiltration systems, such as land use (e.g. Tedoldi et al., 2017; Kluge et al., 2018) and vehicular traffic (e.g. Horstmeyer et al., 2016); provided detailed soil metal contamination spatial patterns (e.g. Tedoldi et al., 2017); and assessed the effects of accumulated metals on lifetime expectancies of the systems (e.g. Ingvertsen et al., 2012). A few studies have evaluated longer term metal accumulation (e.g. Ingvertsen et al., 2012, Horstmeyer et al., 2016), but overall soil metal contamination in biofiltration systems over long time frames (> 10 years), including the potential consequences to biota and to soil management, is insufficiently understood (Tedoldi et al., 2016). To further assess potential effects on soil biota, studies should also evaluate available metal species, such as free metal cations and soluble organic and inorganic metal complexes (Young, 2013), which are more likely to interact with living organisms (Adriano, 2001). Plants and microorganisms can acquire available metal species from the soil solution; if metal concentrations are high enough, this may result in toxic effects including reduced biomass and activity in microorganisms (Giller et al., 2009), and oxidative stress damage, leaf chlorosis, poorly developed root systems, and reduced growth in plants (Adriano, 2001). In spite of these potential impacts, readily available metal species are largely uncharacterized in long-term studies of bioinfiltration systems, although they may be of use to evaluate potential ecological risk. The nature and timing of bioinfiltration system maintenance would ideally also consider soil ecological screening levels (Eco-SSLs) that are protective of soil biota. Yet, although past evaluations of metal accumulation in bioinfiltration soils have assessed metal concentrations and estimated the years until Eco-SSLs would be reached (e.g. Johnson and Hunt, 2016; Tedoldi et al., 2017), a clear rationale for prioritizing monitoring of accumulated metals based on drainage area and bioswale characteristics, and for validating future metal accumulation predictions, has not been discussed.

Here, an approach to inform how bioinfiltration systems could be monitored long term to protect environmental and human health is proposed and initially tested. The approach attends to spatial distribution of metals in bioinfiltration systems, focusing on where most metal accumulation is likely to occur so that ecological risk based on total metal concentrations and Eco-SSLs can be performed. The approach was tested for four bioswales of similar age (>14 years), climate and design, but of varying drainage area characteristics. Soils were sampled for metals often associated with stormwater runoff (Cd, Cu, Pb, Zn) (Grant et al., 2003). Future potential soil remediation needs were estimated by predicting annual metal loads and calculating the number of years until Eco-SSLs would be reached. The objectives were to evaluate i) how drainage area characteristics, such as degree of imperviousness and impervious drainage to bioswale area ratios, relate to metal concentrations in established bioswale soils; ii) how soil metal concentrations relate to location within (e.g. side slope vs. basin bed) and along the flow-path of bioswales; iii) how water soluble metals compare to total metals in bioswale soils; and iv) the risks to soil quality and soil biota given measured and future projected metal concentrations, based on comparison to Eco-SSLs. The hypotheses were that i) metal concentrations would exceed reference levels (i.e. those of nearby areas not receiving stormwater runoff from the built environment), and that metal concentrations would be higher in bioswales with more impervious drainage area and higher impervious drainage to bioswale area ratios; ii) metal concentrations would be higher in the basin bed rather than the side slope due to higher sedimentation; iii) metal concentrations would be higher near discrete stormwater runoff inlets due to particle association and sedimentation; iv) water soluble metal concentrations would be low since a high fraction of metals in stormwater runoff (typically 50–90%) are in particulate form (Grant et al., 2003; LeFevre et al., 2015); and v) total metal concentrations in some of the sampled soils would exceed Eco-SSLs. The hypothesized relationships between drainage areas and metal concentrations were observed but, based on those concentrations and predictions of longer-term conditions, these suburban biofilters are not expected to need soil maintenance for decades. This study builds upon previous work by examining the influence of drainage area characteristics on metal concentrations in established bioinfiltration systems, and by identifying metrics that may be predictive of soil metal concentrations.

2. Methods

2.1. Study site and bioswales

The study site, Manzanita Village, is a 4.9 ha residential university student housing complex located on the University of California, Santa Barbara (UCSB) campus, Santa Barbara, CA (N 34°24′32″; W 119°51′ 28″; Fig. S1). The site has a Mediterranean climate influenced by maritime winds, with monthly temperatures averaging 11.4–19.0 °C (NOAA, 2020; recorded at the proximate Santa Barbara Municipal Airport for the years 2002–2019). Rainfall is variable, occurs mostly from November to April and, for the period 2002 to 2015, averaged 378 mm (Santa Barbara County Public Works, 2020; measured at UCSB station no. 200, N 34°24′56″; W 119°50′43″).

The four study bioswales, consisting of shallow basins separated by rock check dams, were constructed in 2001–02, as part of an ecological restoration project. The basins have average slopes of 2%, and range from 4.5 to 6 m long with trapezoidal cross sections of 2.4 m wide at the top narrowing to 1.2 m at the soil bed surface; the ponding and soil depths are approximately 15 cm (Fig. S2) and 0.9 m, respectively (CCBER, 2008). The bioswales are planted with native sedges and rushes, including *Juncus spp*. (e.g. *J. patens, J. mexicanus, J. occidentalis, J.*

phaeocephalus, *J. textilis*) and *Carex spp*. (e.g. *C. praegracilis*), (CCBER, 2008) that are trimmed annually and weeded manually besides receiving routine spot application of glyphosate-based herbicides for weed control (personal communication, Lanes, A., June 26, 2015).

Stormwater runoff into the bioswales originates from rooftops, paved surfaces, lawns and natural soils (Fig. 1). The velocity of runoff from roof downspouts is dampened in cobble drains that are sufficiently coarse such that negligible sedimentation and pollutant removal occur therein. The contributing metal roofs are pitched (2 in 12 slope), and are comprised of aluminum, copper, and galvanized metal. Local seabirds roost on the roofs where they deposit phosphorous-rich guano; ocean aerosols also settle on roofs and thereby deposit nutrients (CCBER, 2008). Runoff from paved surfaces, lawns and natural soils enters diffusely as sheet flow into the bioswales. There are paved service roads adjacent to the bioswales used by electric powered vehicles, bicycles, and foot traffic. The otherwise unfertilized lawns are irrigated during the dry season with reclaimed water, which may be a source of nutrients (SWRCB, 2016; Fruit Growers Lab Inc., 2020) and solids (Table S1). Reclaimed water, sourced from the reclamation facility at the Goleta Sanitary Water Resource Recovery District at Goleta, CA, consists of secondary effluent treated to tertiary standards via flocculation, filtration through anthracite coal, and chlorine disinfection (Goleta Sanitary, 2018).

Reference sites in close proximity (<10 m) to the bioswales, but not receiving stormwater runoff from built infrastructure, were used ($n = 4$) for comparing soil metal concentrations (Fig. S1). The natural soils in the reference sites are poorly draining, classified as Concepcion fine sandy loam (USDA Natural Resource Conservation Service's Hydrologic Soil Group C), and vegetated with native shrubs.

2.2. Delineation and calculation of drainage areas and degree of imperviousness

An original subwatershed map, which was the design basis of the bioswales, identified the delineation of bioswales and bioswale drainage areas (CCBER, 2003). This information was transferred into ArcMap 10.7.1, using the ESRI World Imagery layer as a basemap (ESRI, 2019), and creating shapefiles using the polygon feature to delineate the bioswales and draining areas corresponding to roofs, paved surfaces, lawns and natural soil cover. Projected areas for each of these draining surfaces were obtained from the attribute table using the "calculate geometry" option. Projected areas for the pitched roofs were adjusted using the slope (2 in 12) to estimate a roof slope multiplier of 1.038. All other areas were unmodified since the study site is relatively flat, so that projected areas from aerial images are correct representations of actual areas.

Total drainage area was computed by summing areas for roofs, paved surfaces, lawns, and natural soil cover. Total impervious area (TIA) was calculated as the sum of areas of roofs and paved surfaces. Percent imperviousness was calculated by dividing the TIA by the total drainage area and multiplying by 100. The directly connected impervious area (DCIA) was calculated as the sum of areas of paved surfaces and roofs directly connected by cobble drains to the bioswales. Two metrics linking drainage areas and bioswale areas were computed: the ratio of TIA to bioswale area, and the ratio of DCIA to bioswale area.

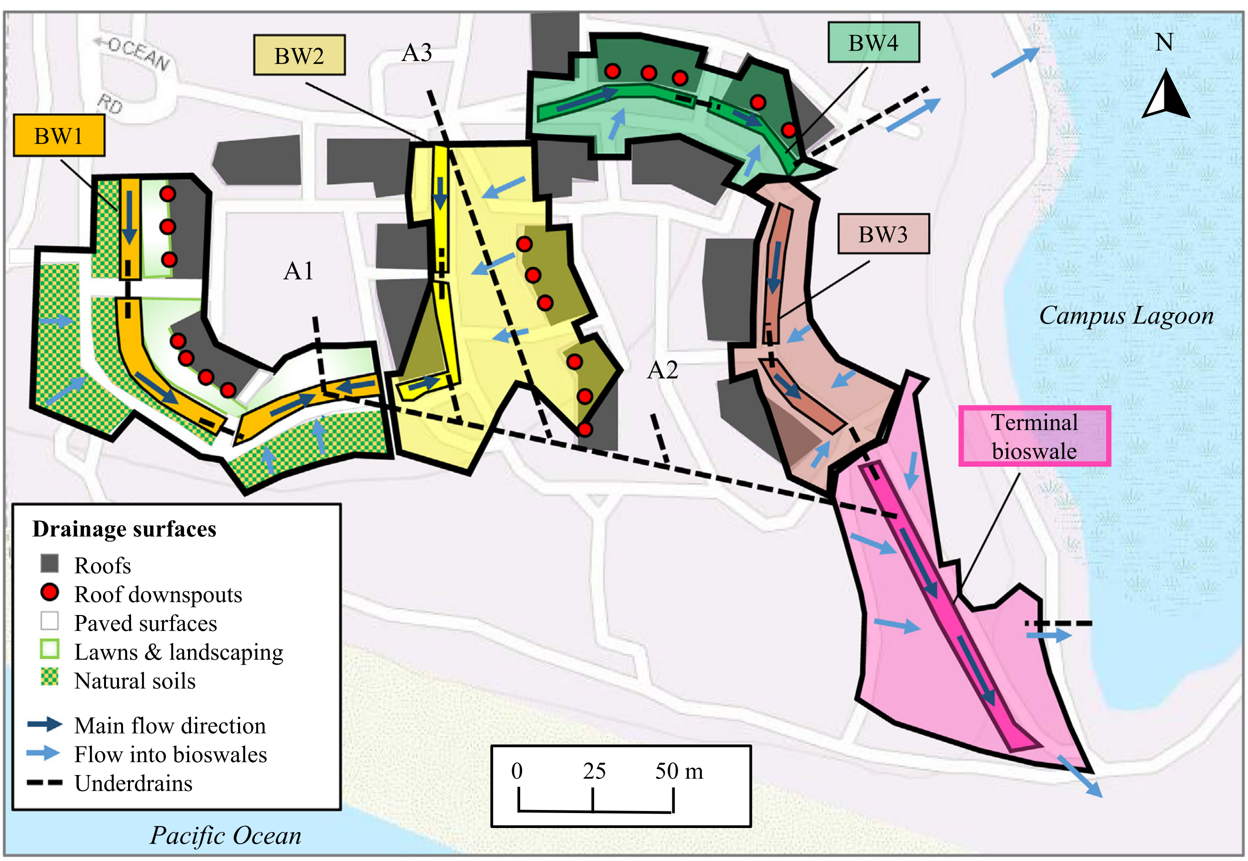

Fig. 1. Schematic of study bioswales (BW1-4) (Fig. S1) and terminal bioswale (not included in study), with the respective drainage areas outlined in black, overlaying a USGS base map (USGS, 2020). Main flow direction in the bioswales is shown as dark arrows. Flows into the bioswales are indicated by light blue arrows. Bioswale segments are connected via underdrains (dashed black lines). At the outlets of BW1, BW2 and BW3, runoff is conveyed via underdrains to a terminal bioswale, which also receives stormwater runoff from zones A1-A3. Final discharges are into the campus lagoon and the beach adjacent to the study site (southeast corner). At the outlet of BW4, an underdrain conveys runoff to a marsh which discharges into the lagoon (northeast corner). For BW1, the delineation of specific drainage areas is shown, including roofs, paved surfaces, lawns and landscaping, and natural soils. For BW2, BW3, and BW4, roofs and roof downspouts within each drainage area are shown. Except for BW1, roof color is in the background when in the drainage area. (For interpretation of the references to color in this figure legend, the reader is referred to the web version of this article.)

2.3. Sampling

Soil sampling occurred between March 21st and April 4th, 2016. Eighteen soil samples were collected per bioswale at nine evenly spaced (9–12 m) locations along the flow-path: nine on the basin bed and nine on the side slope closest to nearby buildings (Fig. S3). Prior to sampling, visible rocks and vegetation were removed from the soil surface. A composite sample of approximately 700 g surface soil (0–10 cm) was obtained from each of three soil cores sampled at each location, using a cylindrical stainless-steel corer (5.08 cm diameter; 20 cm length) and collecting the soil in clean resealable plastic bags. Between uses, the corer was brushed, rinsed with Nanopure water (Barnstead Thermolyne, Ramsey, MN), and dried with a clean cloth. Four reference samples (Fig. S1), indicative of the natural background metal concentrations, were collected in the same way as bioswale soil samples. Samples were maintained on ice (4 °C) until returning to the lab for processing within 6 h. In the lab, the soil samples were sieved (2 mm) and subsampled immediately for analysis.

Additional sampling (four composite samples) to characterize bioswale soils was performed in October 2018. Sieved (2 mm) soil samples were shipped (4 °C) to the Analytical Laboratory of the University of California at Davis (Davis, CA, USA; http://anlab.ucdavis.edu/) where they were analyzed for soil texture (Sheldrick and Wang, 1993), cation exchange capacity (Rible and Quick, 1960), and total N and total C (AOAC, 1997).

2.4. Soil physicochemical characteristics

Gravimetric soil moisture content was determined for triplicate subsamples (3 g) of sieved soil using the mass difference before and after drying (105 °C, 24 h), following standard methods (Gardner, 1986). Dried soils (3 g) from the soil moisture analysis were combusted in a muffle oven at 450 °C for 16 h to determine soil organic matter via loss on ignition (LOI) (Nelson and Sommers, 1996). Soil pH was measured following standard methods (Thomas, 1996), including slurrying soil (10 g soil, 10 g deionized water) and settling the slurry (10 min), then measuring the pH by a pH meter (Oakton Ion 700 benchtop meter; Cole Parmer, Vernon Hills, IL). For inorganic nutrient analysis (nitrate and phosphate), soil samples (3 g, sieved) were extracted with 30 mL of 2 M KCl solution (149 g KCl Certified ACS Fisher Scientific, Pittsburgh, PA in 1 L deionized water) following standard methods (Mulvaney, 1996). Soil extracts were filtered using Whatman quantitative ashless filters, grade 42, 42.5 mm diameter (Sigma-Aldrich, St. Louis, MO) and the filtrate stored (−20 °C) until analysis, within 6 weeks. Filtrates were thawed immediately before analyzing dissolved nitrate and phosphate at the Marine Science Institute (MSI) Analytical Lab at UCSB via flow injection analysis (QuikChem8500 Series 2; Lachat Instruments, Milwaukee, WI). Extraction blanks and filter blanks were included in each inorganic nutrient analysis batch.

2.5. Microbial biomass by substrate induced respiration

The substrate induced respiration (SIR) method, as a metric of soil microbial biomass, was modified from West and Sparling (1986) and Fierer et al. (2003). The measurement was replicated by performing independent measures for each of two duplicate soil samples. To perform, 10 g of composite sieved soil was weighed into individual 250 mL amber glass bottles with Teflon-taped threads, and 10 mL of autoclave-sterilized yeast extract solution (12 g autolyzed BD Difco yeast, BD Biosciences, San Jose, CA in 1 L deionized water) was added. The bottles were capped (Mininert, 24 mm, Valco Instruments Co. Inc., Houston, TX) and placed on a horizontal shaker for the duration of the 4 h incubation. Headspace gas samples (5 mL) were acquired via syringe immediately after capping, then 2 and 4 h thereafter for a total of 3 time-course measurements. To avoid pressure differentials, at each sampling time, 5 mL of air were injected into the sealed bottle via syringe prior to extracting the headspace gas sample. Additional method details are included in Appendix A – Supplementary Information. Gas CO_2 content was measured using an infrared gas analyzer (EGM-4; PP Systems, Amesbury, MA). The slope of CO_2 concentrations against time was used to calculate the rate of CO_2 production, expressed as μg CO_2 x g dry soil^{-1} x h^{-1}.

2.6. Metal analysis

Bioswale soil samples were analyzed for common metals found in stormwater runoff, including Cu, Pb, Zn and also Ni, Cd, and Cr (Grant et al., 2003). Total metals were quantified for strong acid-extracted soils and thus represent "pseudo-total metals", which are those that may become available under worst case environmental conditions (Link et al., 1998), and are thus suited for the scope of this study. Metals that are readily available to plants and microorganisms were evaluated by measuring water soluble metals, based on the method outlined in Seguin et al. (2004) and Rodriguez et al. (2010). To recover eluates for determining water soluble metals, one replicate of 10 g of sieved soil was weighed into 50-mL polypropylene centrifuge tubes with 10 mL chilled (4 °C) distilled water. The samples were vigorously shaken by hand (10 s) and mechanically shaken (2 h, 4 °C) in a controlled environment incubator shaker (New Brunswick Scientific Co. Inc., Edison, NJ) at 4 °C and 200 rpm. The samples were centrifuged (2500 ×g, 30 min, 4 °C) (Cao et al., 2008), and 1 mL of the supernatant was diluted 20-fold in 2% nitric acid (Optima ultrapure grade, Fisher Scientific, Pittsburgh, PA) before storing (4 °C) until analysis (within 4 weeks). Total metal extraction was based on EPA method 3051A and involved weighing sieved soil (one replicate, 0.5 g) into microwave quartz vessels (Anton Paar, Graz, Austria) and digesting (165 °C; 1.0 h) with 16 mL aqua regia (HNO_3 Certified ACS and HCl Certified ACS, Fisher Scientific, Pittsburgh, PA in a 1:3 ratio) in a microwave acceleration reaction system (Multiwave Eco; Anton Paar, Graz, Austria). The digested samples were transferred to acid-rinsed 50 mL PP centrifuge tubes (Corning Life Sciences, Corning, NY) and diluted to 50 mL with Nanopure water (Barnstead Thermolyne, Ramsey, MN). The acid digests were further diluted 9.4 times (1.6 mL acid digest plus 13.4 mL Nanopure water).

Water soluble and total metals were quantified via inductively coupled plasma-atomic emission spectroscopy (ICP-AES) using a TJA High Resolution IRIS instrument (Thermo Electron Corporation, Waltham, MA) based on EPA Methods 200.7 and 6010C, quantifying 11 elements (Al, Ca, Cd, Cr, Cu, Fe, Mg, Mn, Ni, Pb, and Zn) in the solution. Calibration standards were prepared using a commercial standard containing all metals (High-Purity Standard Co., Charleston, SC; 0, 1, 10, and 100 μg/L) in 2% *v*/v nitric acid. Detection limits were 7 μg/L for Pb; 10 μg/L for Cu, Fe, Mn, Zn; 12 μg/L for Mg, Ni; 14 μg/L for Cd and Cr; 22 μg/L for Ca; and 27 μg/L for Al. For quality control, one lab blank (Nanopure water, Barnstead Thermolyne, Ramsey, MN, acidified with concentrated nitric acid, Optima, Fisher Scientific, Pittsburgh, PA), and one lab duplicate were prepared for each extraction batch. Signal drift for the ICP-AES was evaluated with a quality control sample of a known standard injected every ten runs. Samples were measured in triplicate, and the precision of signal measurement expressed as percent relative standard deviation (%RSD) was 0.1–5.0%. Good linearity was observed for all measured metals, with $R^2 > 0.9995$. No trace metals were detected in the lab blanks.

When performing statistical analysis of total Cu data, six samples that were below detection limit (DL = 10 μg/L) were substituted for a value equal to half the detection limit, a method commonly used to address censored data, which can provide an adequate estimate of summary statistics with low bias for data sets with less than 70% censored data (Antweiler and Taylor, 2008).

2.7. Estimation of annual metal loads and years to reach ecological soil screening levels

To simulate potential bioswale soil metal accumulation, average annual metal loads were first estimated using a simplified approach based on the method outlined in Johnson and Hunt (2016) (Eq. (1)), as follows:

$$\text{Annual metal load}\left(\frac{\text{mg metal}}{\text{kg soil}}\right)=\frac{V_R \times C_{M,in} \times \left(1-\frac{M_{rem,\%}}{100}\right)}{\rho_B \times A_{BSW} \times z} \quad (1)$$

where:

V_R = Runoff volume in m^3 (Table S2)
$C_{M,\ in}$ = Mean input metal concentration in mg/m^3 (Tables S3 and S4)
$M_{rem,\ \%}$ = Median percent metal removal for bioswales
ρ_B = measured bulk density of soil media in $kg/m^3 = 1200\ kg/m^3$
A_{BSW} = Surface area of bioswale in m^2 (Table 1)
z = soil depth over which metal concentration was measured in $m = 0.1\ m$

An average median percent removal ($M_{rem,\ \%}$) of 72% for Zn, and 62% for Cu was selected, based on efficiency ratios (ER) for 59 bioswales reviewed by Fardel et al. (2019). The ER estimates overall long-term treatment performance, rather than individual storm events, and is a measure of percent removal based on average inlet and outlet event mean concentrations. Mean input metal concentrations (Cu = 26 mg/m^3; Zn = 159 mg/m^3) were based on stormwater runoff data collected by the Santa Barbara Creeks Division in low impact development (LID) sites in Santa Barbara, CA (Tables S3 and S4). Runoff volumes (V_R) entering each bioswale were calculated via the curve number method outlined in 210-VI-TR-55 (USDA NRCS, 1986), which takes into account relative imperviousness of the drainage area, and characteristics of infiltrating soils. Further details are included in Appendix A – Supplementary Information.

To test the validity of using annual metal loads to simulate metal accumulation in the bioswales, measured and predicted metal concentrations were compared. Predicted concentrations were calculated using annual metal loads, years of operation, and the initial metal concentrations.

Since initial metal concentrations were not measured at the time of construction, concentrations representing the first decile of all measurements, and thus very low contamination levels, were used as a background value for each bioswale, following Tedoldi et al. (2017). Predicted metal concentrations were obtained as the sum of this background concentration and the product of the annual metal load and the number of years in operation. Predicted and measured metal concentrations were compared to Eco-SSLs for Cu (U.S. EPA, 2007a) and Zn (U.S. EPA, 2007b), to determine if levels of ecological concern had been reached. Eco-SSLs are average values based on reviewed ecotoxicity data, representing soil contaminant concentrations protective of four ecological receptors: plants, soil invertebrates, avian wildlife (birds), and mammalian wildlife (mammals). After verifying agreement between predicted and measured metals, metal accumulation into the future was extrapolated to calculate how many years would have to elapse for metal concentrations to reach Eco-SSLs (Eq. (2)), as follows:

$$\text{Years to Eco-SSL} = \frac{\text{Eco-SSL} - \text{Current maximum metal concentration}}{\text{Annual metal load}} \quad (2)$$

2.8. Data analysis

Differences between soil physicochemical characteristics and metal concentrations across bioswales, and differences in metal concentrations between basin bed and side slope samples for each bioswale, were evaluated by one-way analysis of variance on ranks (Kruskal-Wallis) followed by post-hoc Dunn tests ($p < 0.05$) since variables were not normally distributed (Shapiro-Wilk test). Relationships between soil physicochemical characteristics and metal concentrations across all bioswales were evaluated via Spearman rank-order correlations, as were relationships between any significantly varying metal and specific drainage area characteristics. Statistical analyses were performed with R software (version 4.0.1).

Table 1
Characteristics of drainage areas, bioswales, and soils for study bioswales (BW1-4) (Fig. S1).

Characteristics	BW1	BW2	BW3	BW4
Drainage area				
Total Drainage Area (DA) (m^2)	4191	3978	1615	2231
Paved surfaces (%)	19	15	42	28
Rooftops (%)	18	29	11	43
Lawns (%)	27	29	29	18
Natural soils (%)	36	27	18	11
Impervious (%) [a]	37	44	53	71
TIA (m^2) [b]	1586	1756	850	1572
DCIA (m^2) [c]	1586	851	850	1572
Bioswale				
Bioswale Area (m^2)	762	396	345	274
DA/Bioswale Area Ratio	5.5	10.0	4.7	8.1
TIA/Bioswale Area Ratio	2.0	4.5	2.5	5.7
DCIA/Bioswale Area Ratio	2.0	2.2	2.5	5.7
Soil [d]				
Gravimetric Moisture (%)	15.8 (4.5)	21.3 (4.4)	13.6 (2.3)	16.5 (3.9)
Organic Matter (%)	6.6 (3.8)	6.2 (1.1)	6.7 (1.7)	5.9 (2.6)
Nitrate (mg/kg dry soil)	22.5 (14.4)	18.4 (6.4)	6.1 (5.3)	4.2 (3.9)
Phosphate (mg/kg dry soil)	8.0 (6.4)	3.8 (2.9)	1.6 (2.6)	2.7 (1.8)
pH	8.1 (0.4)	8.2 (0.3)	8.0 (0.2)	8.0 (0.3)

[a] Impervious percent calculated as the sum of the percent paved surfaces and rooftops.
[b] TIA = total impervious drainage area (paved surfaces and roofs).
[c] DCIA = directly connected impervious area (paved surfaces and connected roofs).
[d] Values for soil properties include mean and standard deviation ($n = 18$ per bioswale).

3. Results and discussion

3.1. Drainage area delineation and metrics of imperviousness

The delineation of bioswales, their respective drainage areas, and overall stormwater runoff flow direction in the study area are shown over the USGS National map topographic basemap (USGS, 2020) (Fig. 1). Bioswale and total drainage areas ranged from 274 to 762 m^2, and 1615 to 4191 m^2, respectively. Percent imperviousness in bioswale drainage areas ranged from 37 to 71%. Drainage areas in BW1 and BW2 had higher contributions from lawns (27–29%) and natural soils (27–36%), and smaller contributions from paved areas (15–19%), whereas drainage areas in BW3 and BW4 had higher contributions from paved surfaces (42%), and roofs (43%), respectively (Table 1).

Total drainage to bioswale area ratios ranged from 4.7 to 10.0 (Table 1), which is comparable to other bioinfiltration systems: drainage to bioinfiltration area ratios ranged from 8.7 to 53.3 in swales (Tedoldi et al., 2017), and from 3.5 to 14.3 in bioretention cells (Ingvertsen et al., 2012). When considering only impervious drainage area, ratios of TIA to bioswale area ranged from 2.0 to 5.7. The DCIA was equivalent to the TIA for BW1, BW3 and BW4. For BW2, the DCIA excluded roofs not adjacent to the bioswale (Fig. 1). Ratios of DCIA to bioswale area ranged from 2.0 to 5.7 (Table 1).

3.2. Total and water soluble metals

3.2.1. Total metals concentrations and distribution within and across bioswales

Soil metal concentrations in bioinfiltration systems are a reflection of the stormwater runoff inputs, the amount of infiltration, the paths stormwater runoff follows and the extent of settling processes that deposit particles and associated metals (Tedoldi et al., 2017). Bioswale soil samples were tested for metals most often associated with stormwater runoff, including Cu, Pb, Zn and also Ni, Cd, and Cr (Grant et al., 2003). Cd and Pb were below detection limit for all samples. All other metals were

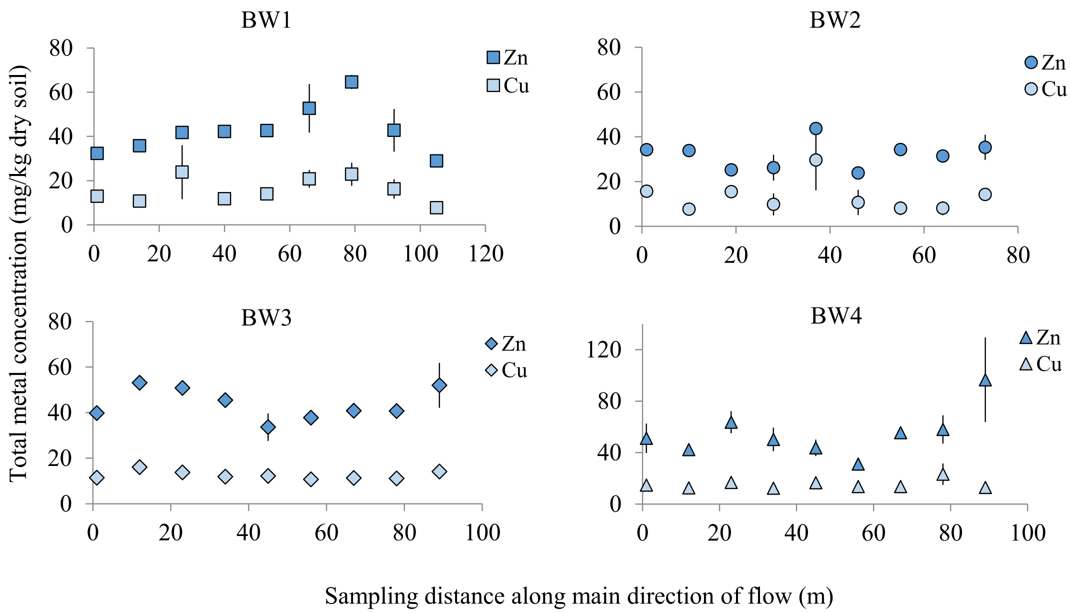

Fig. 2. Total Cu and Zn concentrations in sampled soils along bioswale flow axes. The most upstream sampling location (0 m) is at the north end for BW1, BW2, and BW3, and at the west end for BW4 (Fig. 1). Due to high vegetation density impeding access, the most downstream sampling locations in BW1 and BW2, were 30 m and 15 m in from the east end, and west end, respectively (Fig. 1). Each data point represents the average concentration across one basin bed and one side slope soil sample per sampling location (Fig. S3) for a total of 18 samples per bioswale (BW1-4) (Figs. 1 and S1). Vertical lines show the range of measured concentrations.

detected in a majority of samples, and total Zn was quantified in all samples (Appendix B – Supplementary Data). Within each bioswale, total Zn and total Cu concentrations in basin bed and side slope samples were relatively uniform (Fig. 2), and there were no significant differences for either metal based on location within each bioswale (Kruskal-Wallis, $n = 18$, $p > 0.05$). There were also no clear trends relative to sampling distance along the main direction of stormwater runoff flow (Fig. 2). Previous studies in roadside soils (e.g. Werkenthin et al., 2014) and bioretention cells (e.g. Jones and Davis, 2013, Johnson and Hunt, 2016, Tedoldi et al., 2017) have shown a radial or lateral decrease in metal concentration with distance from the inlet. Due to the multiple inlets in the study bioswales (e.g. roof downspouts and diffuse inputs), such a trend was not observed.

Across all bioswales, total Cu and Zn soil concentrations were low and within the same order of magnitude as reference sites (Kruskal-Wallis, $n = 76$, $p > 0.05$) (Fig. 3a). Metal concentrations in the reference sites were similar to background metal concentrations reported for locations within 100 km of the study site (Appendix B – Supplementary Data). Total Zn concentrations in the study bioswales were 15.6–129.5 mg/kg dry soil, with means of 32.0–54.7 mg/kg dry soil (Figs. 2 and 3a). Total Cu concentrations were above the detection limit (9.4 mg/kg dry soil) in 66 out of 72 bioswale samples and were generally below 20 mg/kg dry soil (Figs. 2 and 3a). Yet there were significant differences across all bioswale samples for Zn (Kruskal-Wallis $\chi2 = 24.284$, $n = 72$, $p < 0.001$). Zn concentrations in BW2 were significantly different from BW1 (Dunn Test, $p = 0.046$), BW3 (Dunn Test, $p = 0.004$) and BW4 (Dunn Test, $p < 0.0001$) (Fig. 2). There were no significant differences for Cu across the bioswales (Kruskal-Wallis $\chi2 = 8.167$, n = 72, $p > 0.05$) (Fig. 3a).

Total Zn and total Cu were significantly correlated across all bioswale samples (Spearman's $\rho = 0.58$, n = 72, $p = 8.5$ E-08) (Fig. S4), which is likely a result of these metals being associated with similar sources in residential areas, such as vehicle use and building materials (e.g. Werkenthin et al., 2014; Charters et al., 2016). Cu and Zn are known

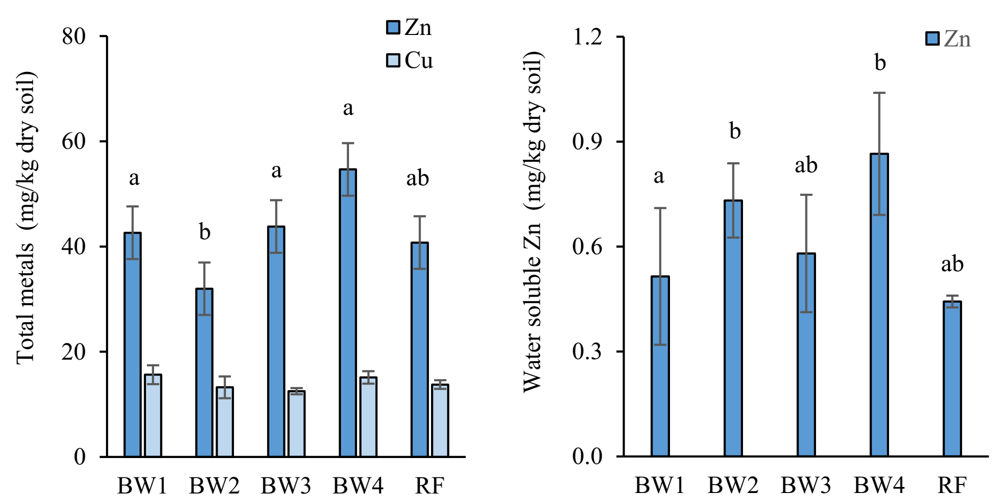

Fig. 3. Total Zn and Cu (a), and water soluble Zn (b) concentrations (mean and standard error) in sampled soils. Means are averages for basin bed and slide slope samples across nine sampling locations (Figs. 2 and S3) for the study bioswales (BW1-4) and four reference soil samples (RF) (Fig. S1). Like letters above the bars denote no significant difference for total or water soluble Zn (Kruskal-Wallis, post-Dunn test, $n = 76$, $\alpha = 0.05$). There were no significant differences for total Cu, and water soluble Cu was below detection limit in all samples.

Table 2
Range of total Cu and Zn soil concentrations for the study bioswales (BW1–4) (Fig. S1) as compared to published data for other bioinfiltration systems, including swales, rain gardens, and bioretention cells.

Bioretention system, runoff type, and soil sampling depth	Age (years)	Total Cu (mg/kg dry soil)	Total Zn (mg/kg dry soil)	Reference
Bioswales, residential, 0–10 cm	>14	10–43	16–130	This study
Swales, parking lot, 0–15 cm	2–10	26–131	66–229	Achleitner et al., 2007
Swales, street and parking lot, 0–3 cm	10–25	20–200 [a]	50–850	Tedoldi et al., 2017
Swales, road, surface, 0–10 cm [b]	ns	2–50	16–565	Liebens, 2001
Swales, road, 0–15 cm	5–15	12–100 [c]	40–400 [c]	Ingvertsen et al., 2012
Swales, roads, topsoil 0–20 cm [a]	1–34	3–730	13–2520	Horstmeyer et al. 2016
Swales, roads and parking lots, 0–10 cm	11–22	6–210	2–1800	Kluge et al., 2018
Bioretention, parking lot, 0–10 cm	3.5–4.5	30–50	80–180	Li and Davis, 2008
Bioretention, parking lot, 0–10 cm	4	8–50	30–250	Jones and Davis, 2013
Bioretention, street and parking lot, 0–10 cm	2–8	5–20	45–88	Paus et al., 2014b
Bioretention, parking lot, 0–5 cm, 5–10 cm	11	2–18	5–228	Johnson and Hunt, 2016

ns: not specified.
[a] Range corresponds to 1st decile and 9th decile.
[b] Liebens (2001) did not specify sampling depth; surface assumed equal to 0–10 cm.
[c] Mean values for studied systems.

to be contributed from metal roofing and siding material via dissolution and degradation (Charters et al., 2016). Relative to published literature on metal accumulation in surface soils of stormwater infiltration systems, total Cu and Zn were within reported ranges for bioinfiltration systems between 2 and 8 years of age, but showed relatively lower metal accumulation than reported for surface soils in residential and parking lot swales aged 6–16 years (Ingvertsen et al., 2012) (Table 2).

The relatively lower total metal concentrations may be a result of low metal loading to the bioswales due to limited vehicular traffic which is a principal contributor of Cu and Zn in stormwater runoff via tire wear and degradation of brake pad linings (Davis et al., 2001; Grant et al., 2003; Charters et al., 2016). Additionally, resuspension and release of previously sequestered pollutants during high flow events may further explain the relatively low measured metal concentrations. Further, leaching down the soil profile due to increases in salinity (e.g. Paus et al., 2014a; Lange et al., 2020), and SOM (e.g. Hatt et al., 2007; Blecken et al., 2011) cannot be excluded, even if studies on lab bioretention columns (e.g. Davis et al., 2001; Hatt et al., 2008) and field bioretention cells (e.g. Li and Davis, 2008; Jones and Davis, 2013) show that soil metal concentrations are higher at the surface. Finally, metal uptake by plants (LeFevre et al., 2015; Muerdter et al., 2018), including phytoextraction and translocation to above ground biomass, or immobilization in roots (Kidd et al., 2009), may contribute to lower soil metal concentrations, even if previous bioinfiltration studies show that some plants play a minor role in metal uptake when compared to soils (e.g. Sun and Davis, 2007; Read et al., 2008; Muerdter et al., 2018). Evaluating the extent of metal accumulation in bioswale vegetation and how plants may influence metal mobility is beyond the scope of this study.

3.2.2. Water soluble metals concentrations and distribution across bioswales

Water soluble Cu concentrations were below detection limit (9.4 mg/kg dry soil) for all samples. Water soluble Zn was measurable in all samples and concentrations were two orders of magnitude lower than total metal concentrations, with values between 0.12 and 3.25 mg/kg dry soil and means of 0.51–0.86 mg/kg dry soil across all bioswales. There were significant differences in water soluble Zn concentrations across sampled soils (Kruskal-Wallis $\chi2 = 20.147$, $n = 76$, $p = 0.0005$) (Fig. 3b), and these differences occurred between BW1 and BW2 (Dunn Test, $p = 0.0004$), and BW1 and BW4 (Dunn Test, $p = 0.0061$).

Unexpectedly, total and water soluble Zn concentrations were weakly and negatively correlated (Spearman's $\rho = -0.34$, $n = 72$, $p = 0.0039$) (Fig. S5). Total metals are often not good predictors of metals in soil solution (Alloway, 2013), which have been shown to positively correlate to metal content in plant tissue (Walker et al., 2003), and in the case of Zn, positively correlate to total Zn content when sorption and mineral dissolution processes dominate over precipitation, as is typical for low Zn loading (Mertens and Smolders, 2013). The low fraction of water soluble metals is not surprising since most metals in soils are either adsorbed to soil particles or present in insoluble forms (Alloway, 2013). Although stormwater runoff carries both dissolved and particulate metals (e.g. LeFevre et al., 2015; Lindfors et al., 2017), dissolved pollutants may rapidly adsorb onto bioswale soil surfaces. Sediment aging, during which metals sorbed on particle surfaces move into smaller pores and voids within the soil matrix, which may not be accessible to living organisms (Alexander, 2000), results in a transfer of metals from labile pools where sorption is reversible to pools where desorption is slow, and further decreases the bioavailability of deposited metals (Mertens and Smolders, 2013).

3.3. Soil physicochemical properties, microbial biomass, and relationships to metals

The bioswale soil was classified as a sandy loam based on particle size analysis (59% sand, 28% silt and 13% clay) (UC Davis, 2018), which is within recommendations for bioinfiltration soils (Geosyntec, 2013). The average cation exchange capacity was 17.6 meq/kg dry soil, total N was 0.2% m/m, and total C was 2.3 m/m (UC Davis, 2018).

Soil pH was determined due to its known influence on metal speciation, solubility and mobility (Young, 2013). The pH was relatively uniform across bioswales (Kruskal-Wallis, $n = 72$, $p > 0.05$), with a range of 7.2–8.6, and means ranging from 8.0 to 8.2 (Table 1). There was no significant correlation between pH and total metal content (Spearman, $n = 72$, $p > 0.05$) (Fig. S5), whereas pH was significantly and negatively correlated to water soluble metals, including Al (Spearman's $\rho = -0.183$, $n = 72$, $p = 0.01$), Fe (Spearman's $\rho = -0.169$, $n = 72$, $p = 0.02$), and Mg (Spearman's $\rho = -0.231$, $n = 72$, $p = 0.01$) (Fig. S5). The soil pH values fall within recommended values for bioinfiltration systems, which range from 5.5 to 8.5 (e.g. Geosyntec, 2011; Geosyntec, 2013; Payne et al., 2015). This pH range supports optimal retention and removal of a broad range of pollutants, including heavy metals, which tend to be immobilized at higher pH (Young, 2013). The relatively high pH in bioswale soils could be a result of the parent soil material used to construct the bioswales, since stormwater runoff is usually neutral in stormwater management systems, as observed in the National Stormwater Quality Database (Pitt et al., 2018). Further, in the study area, runoff has limited contact with surfaces that contribute alkalinity, such as calcareous building materials like concrete pavement (Ingvertsen et al., 2012).

SOM across bioswales was 2.2–14.5% (m/m), with mean values of 5.9–6.7% (m/m) (Table 1). There were no significant differences across bioswales (Kruskal-Wallis, $n = 72$, $p > 0.05$), and SOM content was not significantly correlated with total or water soluble metals (Spearman, n = 72, $p > 0.05$) (Fig. S5). Mean values were within design recommendations for bioinfiltration systems which typically are 5–8% for the soil mix (e.g. State of Washington Department of Ecology, 2019), 10–12% for planting media, and >5% for topsoil (e.g. Geosyntec, 2013). These SOM values could indicate a high affinity to sorb pollutants such as heavy metals due to the presence of humic and fulvic acids (Young, 2013). Conversely, high SOM content can lead to solubilization of organic metal complexes, resulting in metal leaching during runoff infiltration (Davis et al., 2003; Lim et al., 2015), which would result in lower metal concentrations in the upper soil layer.

Nitrate concentrations across the bioswales were 0.9–62.5 mg NO_3/kg dry soil, with means values of 4.2–22.5 mg NO_3/kg dry soil (Table 1). Nitrate concentrations were significantly different across bioswales (Kruskal-Wallis $\chi2 = 44.084$, $n = 72$, $p < 0.001$) and were significantly higher in BW1 and BW2 relative to BW3 and BW4 (Dunn Test, $p < 0.0001$). BW1 and BW2 have larger drainage areas (Table 1) and receive more inputs from irrigation runoff from reclaimed water that is applied to lawns, which may explain the higher soil nutrient content since reclaimed water can potentially contribute nutrients (SWRCB, 2016; Fruit Growers Lab. Inc., 2020). Phosphate concentrations were 0.1–22.8 mg PO_4/kg dry soil, with mean values of 1.6–8.0 PO_4/kg dry soil (Table 1). The mean phosphate concentration was significantly different across bioswales (Kruskal-Wallis $\chi2 = 21.446$, $n = 72$, $p = 0.0065$). Phosphate content in BW1 and BW2 was similar and significantly higher than in BW3 (Dunn Test, $p < 0.05$). BW2 and BW4 had similar phosphate content, as did BW3 and BW4. Phosphate and nitrate were positively correlated (Spearman's $\rho = 0.60$, $n = 72$, $p =$ 7.2E-06) (Fig. S5).

SIR was computed as an indicator of heavy metal stress since high levels of metal pollution can reduce microbial biomass (Giller et al., 2009). There were significant differences across bioswales (Kruskal-Wallis $\chi2 = 30.709$, n = 72, $p =$ 9.8 E-07), with BW3 being higher than BW1, BW2 and BW4 (Dunn Test, $p < 0.05$). SIR values were 1.4–10.0 $\mu g\ CO_2\ g^{-1}\ h^{-1}$, with mean values of 3.7–6.7 $\mu g\ CO_2\ g^{-1}\ h^{-1}$, which are within reported values for semi-arid soils (e.g. Conant et al., 2004). There was no correlation between microbial biomass and total soil metal content across all bioswale samples (Spearman, n = 72, $p > 0.05$). However, SIR was moderately correlated with SOM (Spearman's $\rho = 0.51$, n = 72, $p =$ 4.0 E-06) (Fig. S5), which is expected since SOM is a carbon source for heterotrophic microbial respiration. SIR was also moderately correlated with water soluble metals Al (Spearman's $\rho = 0.52$, n = 72, $p =$ 2.5 E-06), Ca (Spearman's $\rho = 0.43$, n = 72, $p =$ 1.7 E-04), Mg (Spearman's $\rho = 0.54$, n = 72, $p =$ 1.1 E-06), and Fe (Spearman's $\rho = 0.49$, n = 72, $p =$ 1.2 E-05) (Fig. S5).

3.4. Relationship between total metals and drainage area characteristics

Correlations between total Zn and drainage area characteristics were computed to evaluate if the degree of imperviousness in bioswales had an effect on Zn concentrations. Total Zn concentration in bioswale soils was significantly correlated to the contributing drainage basin characteristics of directly connected impervious area to bioswale area ratio (Spearman's $\rho = 0.32$, $n = 71$, $p = 0.0073$), percent impervious cover (Spearman's $\rho = 0.32$, n = 71, p = 0.0073), and paved surfaces (Spearman's $\rho = 0.46$, n = 71, $p =$ 5.6 E-05) (Fig. 4). The correlation between total Zn and the TIA to bioswale area ratio was not significant, which is likely a result of a substantial portion of roof runoff in BW2 flowing through a large lawn area prior to entry into the bioswale (Fig. 1). The DCIA to bioswale area ratio was thus a better predictor for Zn concentrations in bioswale soil. A moderate negative correlation was observed for total Zn and percent lawns (Spearman's $\rho = -0.48$, n = 71, $p =$ 2.4 E-05) (Fig. 4), indicating that these pervious areas may be factors in reducing metal loads to the bioswales. Total Cu showed no significant correlation to surface area characteristics in the drainage area (data not shown), likely as a result of the generally low and uniform observed concentrations.

It should be noted that the positive correlation between total Zn and imperviousness was observed for relatively low Zn concentrations. While not studied here, such correlations might extrapolate upwards. Data reported by Tedoldi et al. (2017), which includes biofiltration systems that receive higher metal loading and/or are much smaller in size relative to their total drainage area, suggests that, on average, soil metal concentrations are higher in systems with larger drainage to bioinfiltration area ratios. However, there may be other site related factors which could obscure this relationship. This study was not confounded by spatial variations in biofilter environmental factors such as local climate, since the four bioswales are in close proximity. Further, the bioswales are similarly designed, were constructed at the same time and thus have similar soil physicochemical characteristics (Table 1). Any differences are likely a result of the types and amount of runoff that the bioswales receive, in addition to differences in vegetation in response to changes in moisture and nutrient inputs. To further test the correlation between accumulated metals and the percent imperviousness in the drainage area, and/or the ratios of impervious drainage to infiltration areas, future studies including a range of bioinfiltration designs and a broader range of impervious drainage to infiltration area ratios will be useful.

3.5. Estimating potential threat and the need for soil media remediation

To evaluate how long it would take for surface soil samples to reach concentrations of potential concern, annual metal loadings were computed and predicted metal concentrations at time of sampling (after 14 years in operation) were calculated, and compared to measured concentrations and to Eco-SSLs. Current maximum metal concentrations were extrapolated into the future to estimate the years until Eco-SSLs would be reached. Annual metal loadings were 1.7–3.1 mg/kg dry soil and 0.2–0.4 mg/kg dry soil, for Cu and Zn respectively (Table 3).

Soil metal concentrations at time of construction, or background metal concentrations, were estimated as the first decile of all measured data at time of sampling, and were 10.0–11.6 mg/kg dry soil and 23.2–37.7 mg/kg dry soil, for Cu and Zn, respectively. These background metal concentrations are within the range observed for surficial (0–5 cm) soils, and below median (Cu: 14.4 mg/kg dry soil; Zn: 58 mg/kg dry soil) and mean (Cu: 17.9 mg/kg dry soil; Zn: 66 mg/kg dry soil) values for soils in the conterminous USA (Smith et al., 2013) (Table 3). Based on background concentrations, annual metal loadings and years in operation, predicted metal concentrations at time of sampling were 12.8–16.7 mg/kg dry soil and 54.6–74.1 mg/kg dry soil, for Cu and Zn respectively. Predicted metal concentrations were comparable to measured Cu concentrations, and larger than measured Zn concentrations (Table 3). Measured Zn concentrations may have been lower than predicted due to source differences between the study site, and the local sites used to estimate Zn concentrations in stormwater runoff, such that the study site had lower Zn loading. It should also be noted that model predictions did not account for future uncertainty in stormwater runoff as a result of climate change, changes in metal loading due to atmospheric deposition inputs, and the role that plants may have in effecting changes in metal mobility in soils. Future model refinement would logically include improvements on metal loading predictions that take into account these factors.

When predicted and measured Cu and Zn concentrations were considered together, there was a significant and positive linear relationship ($R^2 = 0.873$, $p =$ 6.78 E-04, $n = 8$) (Fig. S6). This relationship, though promising, should be tested with a larger number of samples experiencing a broader range of metal concentrations. Notwithstanding, this result suggests that for the studied bioswales, which are impacted by runoff from impervious surfaces (Fig. 4), if initial metal concentrations are known or can be estimated, local data of stormwater runoff metal concentrations, and drainage area characteristics such as percent

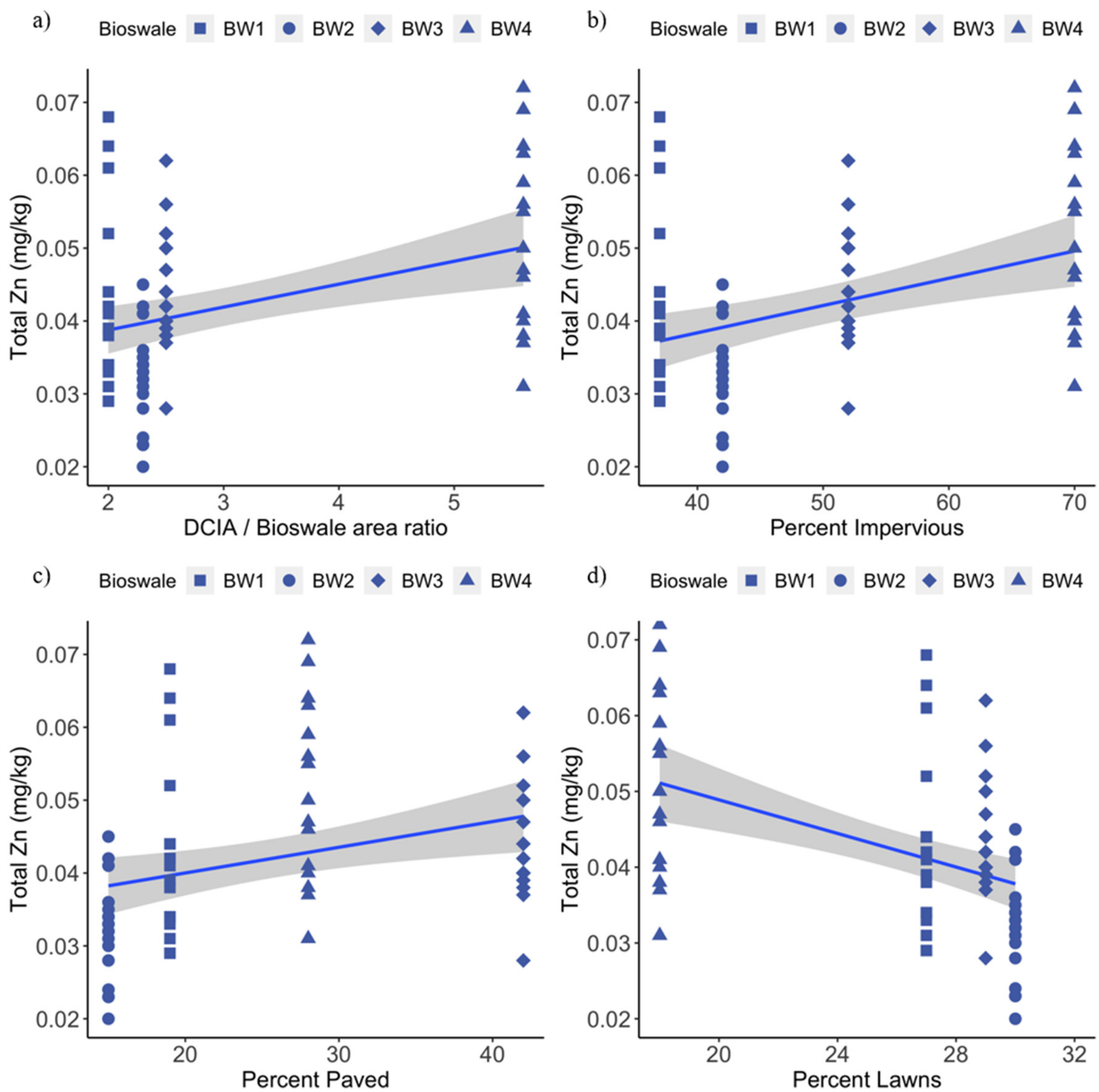

Fig. 4. Spearman correlations between the ranks of total Zn concentration and drainage area characteristics (Table 1) in sampled soils. Results from basin bed and slide slope samples for nine sampling locations (Figs. 2 and S3) for study bioswales (BW1–4) (Fig. S1). One outlier from BW4 has been removed from all data. a) Directly connected impervious area (DCIA) to bioswale area ratio ($\rho = 0.32$, $n = 71$, $p = 0.0073$); b) Percent Impervious ($\rho = 0.32$, n = 71, $p = 0.0073$), c) Percent Paved surfaces ($\rho = 0.46$, $n = 71$, $p = 5.6$ E-05):; and d) Percent Lawns ($\rho = -0.48$, n = 71, $p = 2.4$ E-05). The gray shaded area represents the 95% confidence interval around the line of best fit. Significance level is $\alpha = 0.05$.

Table 3
Background, predicted and measured metal concentrations, annual metal loading, and years until ecological soil screening levels (Eco-SSLs) are reached based on maximum surface (0–10 cm) soil metal concentrations. Annual total metal loadings were calculated by multiplying the estimated average yearly runoff volume entering each bioswale (V_R, Table S2) by the average local metal concentrations in stormwater runoff (Tables S3 and S4). Eco-SSLs are guidance provided by the U.S. EPA, representing concentrations of contaminants protective of four terrestrial ecological receptors: birds, plants, mammals and soil invertebrates (U.S. EPA 2007a).

Parameters	Cu				Zn			
Bioswale	BW1	BW2	BW3	BW4	BW1	BW2	BW3	BW4
Background concentration (mg/kg soil)[a]	10.1	10.0	10.0	11.6	30.4	23.2	37.7	35.6
Annual loading (mg/kg soil per year)	0.23	0.41	0.20	0.36	1.73	3.13	1.53	2.75
Predicted concentration (mg/kg soil)[b]	13.3	15.7	12.8	16.7	54.6	67.1	59.1	74.1
Mean concentration (mg/kg soil)[c]	15.9	14.6	12.5	15.2	42.6	32.0	43.8	54.7
Maximum concentration (mg/kg soil)	36.0	43.2	19.4	31.6	67.8	45.2	61.8	129.5
Years to low Eco-SSL[d]	0	0	43.2	0	0	0.3	0	0
Years to high Eco-SSL[e]	195.3	90.5	10.0	135.7	53.2	36.7	64.2	11.1

[a] At time of construction, estimated from first decile data of measured metals.
[b] After 14 years in operation, based on initial or background concentrations and annual metal loading.
[c] Based on actual concentrations in sampled soils.
[d] Low and high Eco-SSL are 28 mg/kg soil (birds) and 80 mg/kg soil (invertebrates), respectively (U.S. EPA, 2007a).
[e] Low and high Eco-SSL are 46 mg/kg soil (birds) and 120 mg/kg soil (plants), respectively (U.S. EPA, 2007b).

imperviousness, may be used to estimate annual metal loads; metal concentrations can then be projected into the future to evaluate soil ecological risks.

Predicted metal concentrations after 14 years in operation were below all Eco-SSLs for Cu, and above at least one Eco-SSL for Zn for all study bioswales (Table 3). Total and water soluble average metal concentrations measured in the bioswales fell below most Eco-SSLs (Fig. 3, Table 3). When considering maximum concentrations, low Eco-SSLs have been reached in all bioswales in at least one location, either for Cu only, Zn only, or both Cu and Zn (Table 3, Fig. 3a). Current maximum metal concentrations were extrapolated into the future to determine the years until Eco-SSLs would be reached. All bioswales are decades away from reaching high Eco-SSLs (Table 3). Due to the inherent spatial heterogeneity in soil (Young, 2013), the existence of hot spots of contamination that exceed sediment/soil quality guidelines is not overruled, but unlikely in the studied systems where the potential for toxicity to microbes or other soil biota due to accumulated metals is likely minimal.

4. Conclusions

Here, for four lightly metal-contaminated suburban bioswales, which are representative of typical bioinfiltration systems, an approach that unites bioswale drainage area and bioswale characteristics is proposed, which owing to correlations with the highest concentration metal (Zn) (Fig. 4), shows that the two types of characteristics might be predictive of metal loadings, assuming similar compositional drainage area surfaces. The validity of this approach, including extrapolation of current metal concentrations into the future, was verified by the good agreement between predicted metal concentrations based on local stormwater runoff metal concentrations from hardscape and calculated runoff (Table S2), and measured concentrations after 14 years in operation (Table 3, Fig. S6). Notwithstanding, further validation with a larger number of bioinfiltration systems experiencing a range of metal loading is required to fully test the applicability of the proposed strategy for monitoring metals in bioinfiltration soils.

For more contaminated drainage areas and bioswales, e.g. in urban settings, such relationships would be driven by higher magnitudes of metals, imperviousness, and presumably accumulation in the bioswales. However, the extrapolation of these findings to more developed areas remains to be tested. Still, this work suggests that, for other bioswale systems, a reasonable strategy for managing soils to protect resident biota could be to characterize bioswale and drainage areas relative to one another, calculate key indicators from those relationships such as DCIA to bioswale area ratios, then prioritize sampling around higher ratios, compare measured and predicted metal concentrations based on annual metal loads, and assess the trajectory to concerning Eco-SSLs (Fig. 5).

CRediT authorship contribution statement

Marina Feraud: Conceptualization, Methodology, Formal analysis, Investigation, Writing - original draft, Writing - review & editing, Visualization, Supervision, Project administration, Funding acquisition. **Patricia A. Holden:** Conceptualization, Methodology, Writing - review & editing, Supervision, Funding acquisition.

Declaration of competing interest

The authors declare that they have no known competing financial interests or personal relationships that could have appeared to influence the work reported in this paper.

Acknowledgements

Funding for this research was provided by a gift from Mr. Henry H. Wheeler. Additional funding was provided by the UCSB Associated Students Coastal Fund (grant Fall 14-11), and Graduate Summer Fellowships from the Earth Research Institute. The writing of this manuscript was supported by funding from by the University of California Office of the President, Multicampus Research Programs and Initiatives, Grant ID MRP-17-455083. We thank Lisa Stratton, Andy Lanes, Patrick

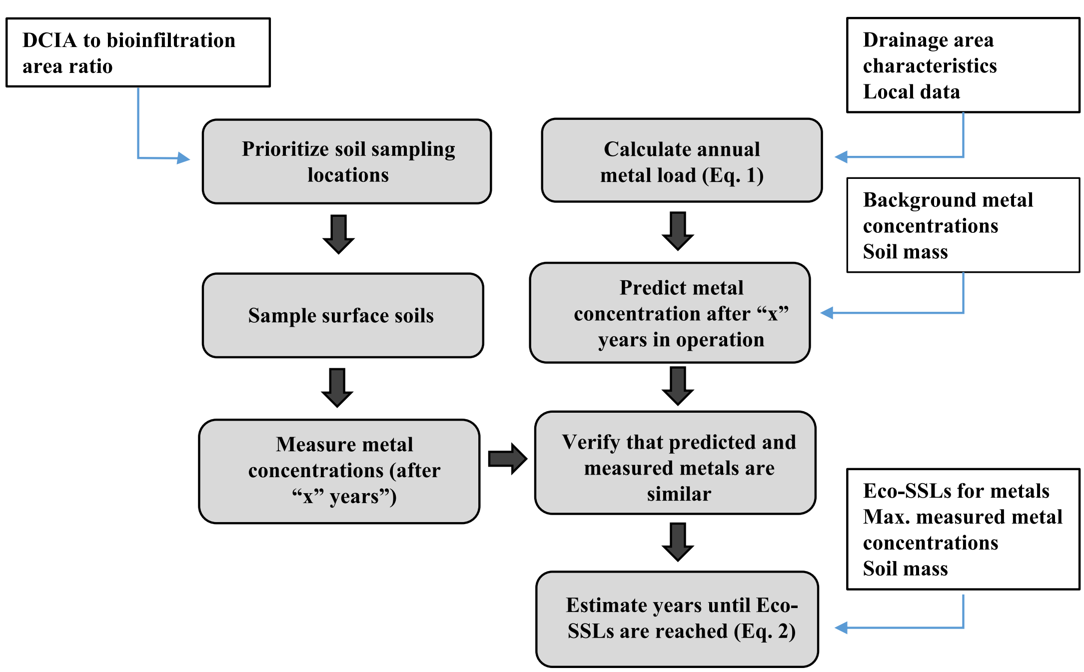

Fig. 5. Proposed strategy to manage soils to protect resident soil biota. The approach includes prioritizing sampling locations for metal analysis based on the ratio of DCIA to bioinfiltration area, calculating annual metal load to predict current soil metal concentrations, comparing predicted and measured concentrations, and projecting future metal concentrations to estimate years until Eco-SSLs are reached. Inputs required to compute the annual metal load are local data of annual precipitation and metal concentrations in stormwater runoff, and drainage area characteristics such as infiltrating soil type, percent vegetation cover, percent impervious drainage, and total drainage area. To estimate the soil mass accumulating metals, inputs are bioinfiltration area, soil depth, and bulk density. Trajectory to Eco-SSLs is estimated based on maximum metal concentrations to represent conservative estimates.

Roehrdanz. Laurie Van der Werfhorst, Sage Davis, Do Gyun Lee, Monika Mortimer, Ying Wang, Timnit Kefela, Cruz Ortiz, Tania Gomez Ayala, and Manu Chopra for their assistance. The MRL Shared Experimental Facilities were used for ICP-AES, and are supported by the MRSEC Program of the NSF under Award No. DMR 1121053, a member of the NSF-funded Materials Research Facilities Network (www.mrfn.org).

Appendix A. Supplementary data

Supplementary data to this article can be found online at https://doi.org/10.1016/j.scitotenv.2020.143778.

References

Achleitner, S., Engelhard, C., Stegner, U., Rauch, W., 2007. Local infiltration devices at parking sites – experimental assessment of temporal changes in hydraulic and contaminant removal capacity. Water Sci. Technol. 55 (4), 193–200.
Adriano, D.C., 2001. Trace Elements in Terrestrial Environments: Biogeochemistry, Bioavailability and Risks of Metals. 2nd edition. Springer-Verlag, New York.
Ahiablame, L.M., Engel, B.A., Chaubey, I., 2012. Effectiveness of low impact development practices: literature review and suggestions for future research. Water, Air, & Soil Pollut 223 (7), 4253–4273.
Alexander, M., 2000. Aging, bioavailability, and overestimation of risk from environmental pollutants. Environ. Sci. Technol. 34 (20), 4259–4265.
Alloway, B., 2013. Sources of heavy metals and metalloids in soils. In: Alloway, B. (Ed.), Heavy Metals in Soils: Trace Metals and Metalloids in Soils and their Bioavailability, 3rd edition Springer, Dordrecht, Netherlands, pp. 11–50.
Ambrose, R.F., Winfrey, B.K., 2015. Comparison of stormwater biofiltration systems in Southeast Australia and Southern California. Wiley Interdiscip. Rev. Water 2 (2), 131–146.
Antweiler, R.C., Taylor, H.E., 2008. Evaluation of statistical treatments of left-censored environmental data using coincident uncensored data sets: I. Summary statistics. Environ. Sci. Technol. 42 (10), 3732–3738.
Association of Official Analytical Chemists (AOAC), 1997. Official method 972.43, microchemical determination of carbon, hydrogen, and nitrogen. Official Methods of Analysis of AOAC International, 16th ed. AOAC International, Arlington, VA (-Chapter 12, 5 – 6).
Blecken, G.T., Zinger, Y., Deletić, A., Fletcher, T.D., Viklander, M., 2009. Impact of a submerged zone and a carbon source on heavy metal removal in stormwater biofilters. Ecol. Eng. 35 (5), 769–778.
Blecken, G., Marsalek, J., Viklander, M., 2011. Laboratory study of stormwater biofiltration in low temperatures: Total and dissolved metal removals and fates. Water Air Soil Pollut. 219 (1–4), 303–317.
Boehm, A.B., Bell, C.D., Fitzgerald, N.J.M., Gallo, E., Higgins, C.P., Hogue, T.S., Luthy, R.G., Portmann, A.C., Ulrich, A.B., Wolfand, J.M., 2020. Biochar-augmented biofilters to improve pollutant removal from stormwater – can they improve receiving water quality? Environ. Sci.: Water Res. Technol. 6, 1520–1537.
Cao, Y., Green, P.G., Holden, P.A., 2008. Microbial community composition and denitrifying enzyme activities in salt marsh sediments. Appl. Environ. Microbiol. 74 (24), 7585–7595.
Charters, F.J., Cochrane, T.A., O'Sullivan, A.D., 2016. Untreated runoff quality from roof and road surfaces in a low intensity rainfall climate. Sci. Tot. Environ. 550, 265–272.
Cheadle Center for Biodiversity and Ecological Restoration (CCBER), 2003. Subwatershed Map for Manzanita Village Project Site. University of California, Santa Barbara, CA.
Cheadle Center for Biodiversity and Ecological Restoration (CCBER), 2008. 5 Year Performance Criteria Monitoring Report for Restored Wetlands at Manzanita Village. University of California, Santa Barbara, CA.
Conant, R.T., Dalla-Betta, P., Klopatek, C.C., Klopatek, J.M., 2004. Controls on soil respiration in semiarid soils. Soil Biol. Biochem. 36 (6), 945–951.
Davis, A.P., Shokouhian, M., Ni, S., 2001. Loading estimates of lead, copper, cadmium, and zinc in urban runoff from specific sources. Chemosphere 44 (5), 997–1009.
Davis, A.P., Shokouhian, M., Sharma, H., Minami, C., Winogradoff, D., 2003. Water quality improvement through bioretention: lead, copper, and zinc removal. Water Environ. Res. 75 (1), 73–82.
ESRI, 2019. ArcGIS Desktop: Release 10.7. Environmental Systems Research Institute, Redlands, CA.
Fardel, A., Peyneau, P.E., Béchet, B., Lakel, A., Rodriguez, F., 2019. Analysis of swale factors implicated in pollutant removal efficiency using a swale database. Environ. Sci. Pollut. Res. 26, 1287–1302.
Fierer, N., Schimel, J.P., Holden, P.A., 2003. Variation in microbial community composition through two soil depth profiles. Soil Biol. Biochem. 35, 167–176.
Fruit Growers Lab Inc., 2020. General Irrigation Suitability Analysis, Reclaimed Water Sampled on July 15th, 2020. Lab IDs SP 2009363–005, and SP 2009363-006.
Gardner, W.H., 1986. Water content. In: Klute, A. (Ed.), Methods of Soil Analysis, Part 1, Physical and Mineralogical Methods, 2nd edition Agronomy Monographs vol. 9(1). American Society of Agronomy, Madison, WI, pp. 493–544.
Geosyntec Consultants (2013). City of Santa Barbara Stormwater BMP Guidance Manual, July 2013 (Final), Section 6.6.2 Vegetated Swale Filter, p. 6–45, accessed on 06/28/2020, https://www.santabarbaraca.gov/civicax/filebank/blobdload.aspx?BlobID=16665
Geosyntec Consultants and Larry Walker Associates (2011). Ventura County technical guidance manual for stormwater quality control measures. Manual Update 2011, Errata Update 2018. Section 6.3, BIO-3: Vegetated Swale, p. 6–149, accessed on 06/28/2020, http://www.vcstormwater.org/images/stories/NPDES_Documents/TGM/TGM_2018_Errata/Ventura-Technical-Guidance-Manual-Rev-06_29_18.pdf
Giller, K.E., Witter, E., McGrath, S.P., 2009. Heavy metals and soil microbes. Soil Biol. Biochem. 41, 2031–2037.
Goleta Sanitary District (2018). 2017 reclaimed water annual report. Accessed on 08/23/20, available at https://goletasanitary.org/downloads/category/11-reclaimed-water
Grant, S.B., Rekhi, N.V., Pise, N.R., Reeves, R.L., 2003. A Review of the Contaminants and Toxicity Associated with Particles in Stormwater Runoff. CTSW-RT-03-059.73.15. Prepared for California Department of Transportation. August 2003.
Hatt, B.E., Fletcher, T.D., Deletic, A., 2007. Hydraulic and pollutant removal performance of stormwater filters under variable wetting and drying regimes. Water Sci. Technol. 56 (12), 11–19.
Hatt, B.E., Fletcher, T.D., Deletic, A., 2008. Hydraulic and pollutant removal performance of fine media stormwater filtration systems. Environ. Sci. Technol. 42 (7), 2535–2541.
Hatt, B.E., Fletcher, T.D., Deletic, A., 2009. Hydrologic and pollutant removal performance of stormwater biofiltration systems at the field scale. J. Hydrol. 365 (3), 310–321.
Horstmeyer, N., Huber, M., Drewes, J.E., Helmreich, B., 2016. Evaluation of site-specific factors influencing heavy metal contents in the topsoil of vegetated infiltration swales. Sci. Tot. Environ. 560–561, 19–28.
Ingvertsen, S.T., Cederkvist, K., Regent, Y., Sommer, H., Magid, J., Jensen, M.B., 2012. Assessment of existing roadside swales with engineered filter soil: I. Characterization and lifetime expectancy. J. Environ. Qual. 41 (6), 1960–1969.
Johnson, J.P., Hunt, W.F., 2016. Evaluating the spatial distribution of pollutants and associated maintenance requirements in an 11 year-old bioretention cell in urban Charlotte, NC. J. Environ. Manag. 18 (2), 363–370.
Jones, P.S., Davis, A.P., 2013. Spatial accumulation and strength of affiliation of heavy metals in bioretention media. J. Environ. Eng. 139, 479–487.
Kidd, P., Barceló, J., Bernal, M.P., Navari-Izzo, F., Poschenrieder, C., Shileve, S., Clemente, R., Monterroso, C., 2009. Trace element behaviour at the root–soil interface: implications in phytoremediation. Environ. Exp. Bot. 67, 243–259.
Kluge, B., Markert, A., Facklam, M., Sommer, H., Kaiser, M., Pallasch, M., Wessolek, G., 2018. Metal accumulation and hydraulic performance of bioretention systems after long-term operation. J. Soils Sediments 18, 431–441.
Lange, K., Österlund, H., Viklander, M., Blecken, G.T., 2020. Metal speciation in stormwater bioretention: removal of particulate, colloidal and truly dissolved metals. Sci. Tot. Environ. 734, 138121.
LeFevre, G.H., Paus, K.H., Natarajan, P., Gulliver, J.S., 2015. Review of dissolved pollutants in urban storm water and their removal and fate in bioretention cells. J. Env. Eng. 141 (1), 0401 4050.
Li, H., Davis, A.P., 2008. Heavy metal capture and accumulation in bioretention media. Environ. Sci. Technol. 42 (14), 5247–5253.
Liebens, J., 2001. Heavy metal contamination of sediments in stormwater management systems: the effect of land use, particle size, and age. Environ. Geol. 41 (3–4), 341–351.
Lim, H.S., Lim, W., Hu, J.Y., Ziegler, A., Ong, S.L., 2015. Comparison of filter media materials for heavy metal removal from urban stormwater runoff using biofiltration systems. J. Environ. Manag. 147, 24–33.
Lindfors, S., Österlund, H., Viklander, M., 2017. Truly dissolved and labile cu and Zn in urban runoff from a parking lot, an industrial area and copper and zinc roofs. 14th IWA/IAHR International Conference on Urban Drainage: Conference Proceedings, Prague, Czech Republic.
Link, D.D., Walter, P.J., Kingston, H.M., 1998. Development and validation of the new EPA microwave-assisted leach method 3051A. Environ. Sci. Technol. 32 (22), 3628–3632.
Mertens, J., Smolders, E., 2013. Chapter 17, Zinc. In: Alloway, B. (Ed.), Heavy Metals in Soils: Trace Metals and Metalloids in Soils and their Bioavailability, 3rd edition Springer, Dordrecht, Netherlands, pp. 465–493.
Miller, J.D., Kim, H., Kjeldsen, T.R., Packman, J., Grebby, S., 2014. Assessing the impact of urbanization on storm runoff in a peri-urban catchment using historical change in impervious cover. J. Hydrol. 515, 59–70.
Mohanty, S.K., Valenca, R., Berger, A.W., Yu, I.K.M., Xiong, X., Saunders, T.M., Tsang, T.C.W., 2018. Plenty of room for carbon on the ground: potential applications of biochar for stormwater treatment. Sci. Tot. Environ. 625, 1644–1658.
Muerdter, C.P., Wong, C.K., LeFevre, G., 2018. Emerging investigator series: the role of vegetation in bioretention for stormwater treatment in the built environment: pollutant removal, hydrologic function, and ancillary benefits. Environ. Sci.: Water Res. Technol. 4, 592–612.
Mulvaney, R.L., 1996. Nitrogen – inorganic forms. In: Sparks, D.L. (Ed.), Methods of Soil Analysis, Part 3 – Chemical Methods. SSSA Book Series No. 5. Soil Science Society of America, Madison, WI, pp. 1129–1131.
National Climatic Data Center (2020). Climate data online search, Global summary of the year for Santa Barbara Municipal Airport, CA, US station, accessed on 06/212020, https://www.ncdc.noaa.gov/cdo-web/datasets/GSOY/stations/GHCND:USW00023190/detail
National Research Council, 2009. Urban Stormwater Management in the United States. The National Academies Press, Washington, DC.
Nelson, D.W., Sommers, L.E., 1996. Total carbon, organic carbon, and organic matter. In: Sparks, D.L. (Ed.), Methods of Soil Analysis, Part 3 – Chemical Methods. SSSA Book Series No. 5. Soil Science Society of America, Madison, WI, pp. 1002–1005.
Paus, K.H., Morgan, J., Gulliver, J.S., Leiknes, T., Hozalski, R.M., 2014a. Effects of temperature and NaCl on toxic metal retention in bioretention media. J. Environ. Eng. 140 (10), 04014034.
Paus, K.H., Morgan, J., Gulliver, J.S., Leiknes, T., Hozalski, R.M., 2014b. Assessment of the hydraulic and toxic metal removal capacities of bioretention cells after 2 to 8 years of service. Water Air Soil Pollut. 225, 1803.

Payne, E.G., Hatt, B.E., Deletic, A., Dobbie, M.F., McCarthy, D.T., Chandrasena, G.I., 2015. Adoption Guidelines for Stormwater Biofiltration Systems – Summary Report. Cooperative Research Centre for Water Sensitive Cities, Melbourne, Australia.

Pitt, R., Maestre, A., Clary, J., 2018. The National Stormwater Quality Database (NSQD, Version 4.02). https://www.bmpdatabase.org/nsqd.html. (Accessed 28 June 2020).

Read, J., Wevill, T., Fletcher, T., Deletic, A., 2008. Variation among plant species on pollutant removal from stormwater non biofiltration systems. Water Res. 42 (4–5), 893–902.

Rible, J.M., Quick, J., 1960. Method S-19.0. Cation exchange capacity. Water Soil Plant Tissue. Tentative Methods of Analysis for Diagnostic Purposes. University of California Agricultural Experiment Service, Davis (Mimeographed Report).

Rodriguez, S.M., Henriques, B., Coimbra, J., Kilburn, J.E., Fey, D.L., 2010. Water-soluble fraction of mercury, arsenic and other potentially toxic elements in highly contaminated sediments and soils. Chemosphere 78, 1301–1312.

Santa Barbara County of Public Works – Flood Control District (2020). Monthly and yearly rainfall record, station: 200, station name: UCSB, accessed on 06/28/2020, http://cosb.countyofsb.org/pwd/water/downloads/hydro/200dailys.pdf

Seguin, V., Gagnon, C., Courchesne, F., 2004. Changes in water extractable metals, pH and organic carbon concentrations at the soil-root interface of forested soils. Plant Soil 260, 1–17.

Sheldrick, B.H., Wang, C., 1993. Particle-size distribution. In: Carter, M.R. (Ed.), Soil Sampling and Methods of Analysis. Canadian Society of Soil Science, Lewis Publishers, Ann Arbor, MI, pp. 499–511.

Smith, D.B., Cannon, W.F., Woodruff, L.G., Solano, F., Kilburn, J.E., Fey, D.L., 2013. Geochemical and Mineralogical Data for Soils of the Conterminous United States: U.S. Geological Survey Data Series 801. 19 p. https://pubs.usgs.gov/ds/801/.

State of Washington Department of Ecology, 2019. Stormwater Management Manual for Western Washington. Publication No.19-10-021.

State Water Resources Control Board (2016). WQ 2016-0068-DDW. Water reclamation requirements for recycled water use, accessed on 06/28/2020, https://www.waterboards.ca.gov/board_decisions/adopted_orders/water_quality/2016/wqo2016_0068_ddw.pdf

Sun, X., Davis, A.P., 2007. Heavy metal fates in laboratory bioretention systems. Chemosphere 66 (9), 1601–1609.

Tedoldi, D., Chebbo, G., Pierlot, D., Kovacs, Y., Gromaire, M.C., 2016. Impact of runoff infiltration on contaminant accumulation and transport in the soil/filter media of sustainable urban drainage systems: a literature review. Sci. Total Environ. 569–570, 904–926.

Tedoldi, D., Chebbo, G., Pierlot, D., Branchu, P., Kovacs, Y., Gromaire, M.C., 2017. Spatial distribution of heavy metals in the surface soil of source-control stormwater infiltration devices – inter-site comparison. Sci. Total Environ. 579, 881–892.

Thomas, G.W., 1996. Soil pH and soil acidity. In: Sparks, D.L. (Ed.), Methods of Soil Analysis, Part 3 – Chemical Methods. SSSA Book Series No. 5. Soil Science Society of America, Madison, WI, pp. 475–490.

U.S. Department of Agriculture (1986). Urban Hydrology for Small Watersheds. Technical Release 55, 210-VI-TR-55, Second Ed., Chapter 2, accessed on 07/04/2020, available at https://www.nrcs.usda.gov/Internet/FSE_DOCUMENTS/stelprdb1044171.pdf

U.S. Environmental Protection Agency (2007a). Ecological Screening Levels for Copper. Interim Final. OSWER Directive 9285.7–68. Washington, DC: USEPA, accessed 06/28/2020, https://rais.ornl.gov/documents/eco-ssl_copper.pdf

U.S. Environmental Protection Agency (2007b). Ecological Screening Levels for Zinc. Interim Final. OSWER Directive 9285.7-73. Washington, DC: USEPA, accessed 06/28/2020, https://rais.ornl.gov/documents/eco-ssl_zinc.pdf

UC Davis Analytical Lab 2018, work request number 19S087, samples 1-4, accessed on 07/04/20 at https://anlab.ucdavis.edu/Results/Link/8c2afe47-3616-4738-9135-ab987c2ed980.

USGS (2020). The National Map. Sources: Esri, HERE, Garmin, Intermap, increment P Corp., GEBCO, USGS, FAO, NPS, NRCAN, GeoBase, IGN, Kadaster NL, Ordnance Survey, Esri Japan, METI, Esri China (Hong Kong), (c) OpenStreetMap contributors, and the GIS User Community.

Walker, D.J., Clemente, R., Roig, A., Bernal, M.P., 2003. The effects of soil amendments on heavy metal bioavailability in two contaminated Mediterranean soils. Environ. Pollut. 122 (2), 303–312.

Werkenthin, M., Kluge, B., Wessolek, G., 2014. Metals in European roadside soils and soil solution – a review. Environ. Pollut. 189, 98–110.

West, A., Sparling, G., 1986. Modifications to the substrate-induced respiration method to permit measurement of microbial biomass in soils of differing water contents. J. Microbiol. Methods 5, 177–189.

Young, S.D., 2013. Chemistry of heavy metals and metalloids in soils. In: Alloway, B. (Ed.), Heavy Metals in Soils. Environmental Pollution. vol 22. Springer, Dordrecht, Netherlands, pp. 51–95.

Appendix A - Supplementary Information for

Evaluating the relationships between specific drainage area characteristics and soil metal concentrations in long-established bioswales receiving suburban stormwater runoff

Marina Feraud[1,2], and Patricia Holden[1,2]

1 Bren School of Environmental Science and Management, University of California, Santa Barbara, CA 93106, United States.

2 Earth Research Institute, University of California, Santa Barbara, CA 93106, United States.

*Corresponding Author: mferaud@bren.ucsb.edu, 805-403-3130 (phone).

Number of pages: 15

Number of tables: 4

Number of figures: 6

List of Figures

Figure S1. Aerial image of the Manzanita Village project site.

Figure S2. Photographic example and schematic of study bioswales.

Figure S3. Soil sampling schematic.

Figure S4. Spearman correlation between the ranks of total Cu and Zn for sampled soils.

Figure S5. Spearman correlations between the ranks of physicochemical characteristics and metals in sampled soils.

Figure S6. Comparison between predicted and measured metal concentrations in sampled soils.

List of Tables

Table S1. Characteristics of tertiary treated and disinfected reclaimed water used for lawn irrigation in the study area.

Table S2. Calculation parameters and results for yearly stormwater runoff entering study bioswales BW1-4.

Table S3. Cu concentrations in stormwater runoff entering low impact development sites in Santa Barbara, California.

Table S4. Zn concentrations in stormwater runoff entering low impact development sites in Santa Barbara, California.

Additional Methods

Estimation of runoff volumes to calculate annual metal loads

Runoff volumes entering each bioswale were calculated via the curve number (CN) method outlined in 210-VI-TR-55 (USDA NRCS 1986). Input parameters for the calculation include the yearly average precipitation for the period 2002 – 2015 (378 mm/yr), measured at a weather station close to the site (UCSB; station no. 200; N 34°24’ 56”; W 119°50’43”) (Santa Barbara County Public Works 2020), and appropriate runoff CNs for soils in hydrologic group C, which is representative of soils in the study site. Runoff (Q_R) for each bioswale was calculated as:

$$Q_R\,(\mathrm{mm}) = \frac{(P-I)^2}{P-I+S} = \frac{(P-0.05S)^2}{P+0.95S} \tag{S.1}$$

where

P = precipitation (mm)

S (in) = potential maximum retention after runoff begins (in) = [1000/CN -10]

S (mm) = S(in) x 25.4 mm/in

I = initial abstraction (mm), here defined as I = 0.05S. This is an actualization from the original formula (I = 0.2S), proposed by Woodward et al. (2003) after evaluating runoff-rainfall data from several hundred storm events.

CN = curve number (dimensionless, takes values from 0 to 100)

A composite CN is computed for each bioswale using Fig. 2.3 in 210-VI-TR-55 (USDA NRCS 1986). The directly connected impervious area, which includes paved surfaces and roofs connected to bioswales via cobble drains (Table 1), is used as the x-axis value to read up from until intersecting the appropriate pervious CN curve, and the composite CN value is read across on the y-axis. For the study site, a pervious CN of 74 is selected, corresponding to open space in good condition for soils in hydrologic group C (Table 2.2a in 210-VI-TR-55 (USDA NRCS 1986) (Table S2). The runoff volume (V_R) entering each bioswale (Table S2) is obtained by multiplying the Q_R computed in equation (S.1) by the respective drainage area (Table 1).

Substrate induced respiration (SIR)

The headspace volume in the sealed bottle used for the SIR assay was estimated by subtracting media (10 mL) and soil volumes from the bottle volume (256 mL). Soil volume was estimated from the dry soil weight and a soil bulk density of 1.5 g/cm^3, appropriate for a sandy loam.

To avoid significant pressure differentials during the 3-hour incubation, at each sampling time 5 mL of air were injected into the bottle using a syringe, the headspace was mixed by pumping the syringe three times, and a well-mixed headspace sample (5 mL) was extracted. No overpressure or vacuum was observed during any of the sampling steps. To calculate the actual CO_2 concentration at each sampling point, prior to the addition of 5 mL of air, the law of additive volumes was used, assuming ideal gas behavior, such that:

$$[CO_2]_{actual} = ([CO_2]_{measured} \text{ x } V_{total} - V_{air} * [CO_2]_{air}) \text{ x } V_{headspace}^{-1}$$

Where:

$[CO_2]_{actual}$ is the CO_2 concentration in ppm (v/v), accounting for the air dilution effect

$[CO_2]_{measured}$ is the CO_2 concentration in ppm (v/v), measured by the gas analyzer

V_{total} is the sum of the headspace volume and the air addition volume, in mL

V_{air} is the volume of air addition, which is 5 mL

$V_{headspace}$ is the volume of the bottle minus the volume of soil and media

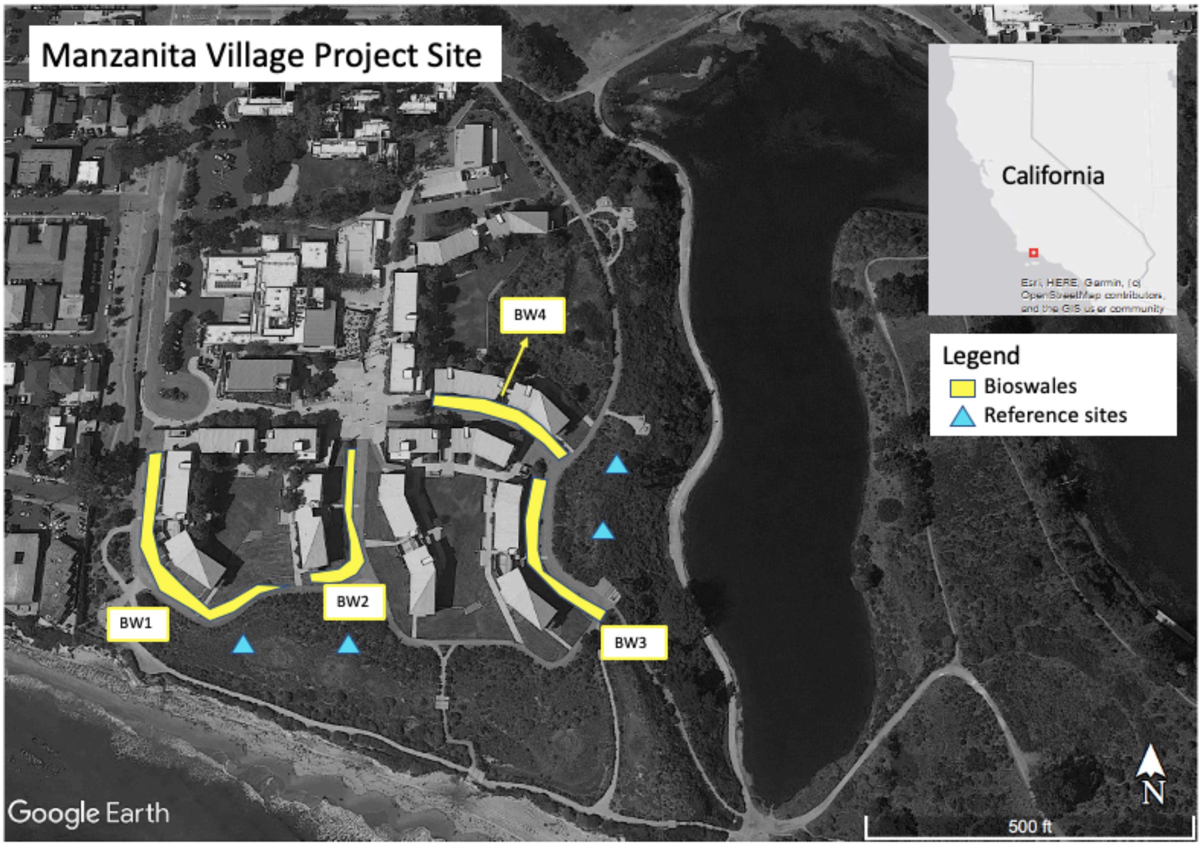

Fig. S1. Aerial image of Manzanita Village project site (N 34°24'32"; W 119°51'28") downloaded on 06/22/2020 from Google Earth. Study bioswales (BW1-4) are delineated in yellow. Reference sites, shown via blue triangles, are areas that are close to the bioswales, and do not receive runoff from built infrastructure.

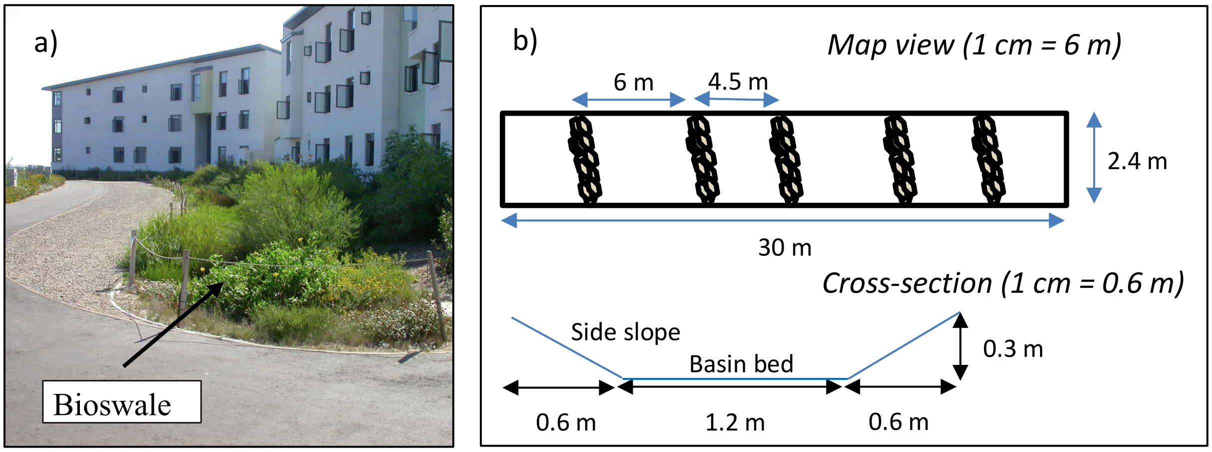

Fig. S2. a) Example photograph of one study bioswale (BW2) (Fig. S1). b) Schematic of bioswale geometry showing plan view (top) of basins separated by rock check dams, and basin cross-section (bottom), with location of basin bed and side slope.

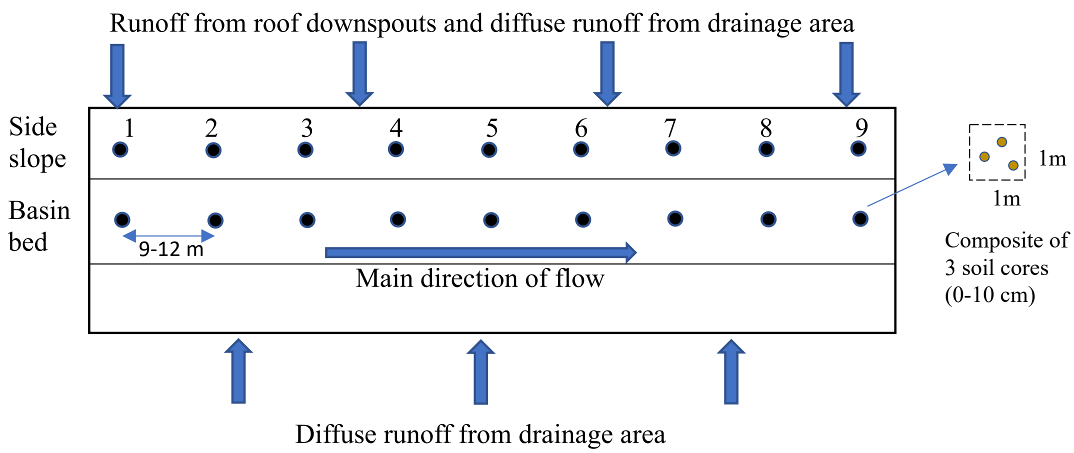

Fig. S3. Soil sampling schematic. Nine locations, equally spaced (9 to 12 meters apart depending on the total length of the bioswale), were chosen to span the length of each bioswale. At each location, soils were sampled from the basin bed and from the side slope, for a total of 18 samples per bioswale. Each sample is a composite of three soil cores, sampled to a depth of 10 cm.

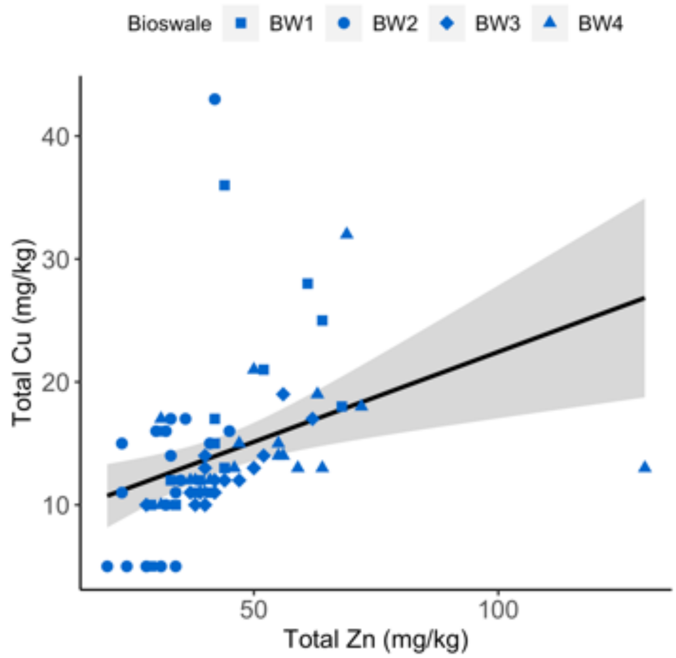

Fig.S4. Spearman correlation between the ranks of total Cu and Zn ($\rho = 0.58$, $n = 72$, $p = 8.5$ E-08) for sampled soils. Plotted data include those from the basin bed and side slope samples from nine sampling locations (Fig. 2) for study bioswales (BW1-4) (Fig. S1). The gray shaded area represents the 95% confidence interval around the line of best fit. Significance level is $\alpha = 0.05$.

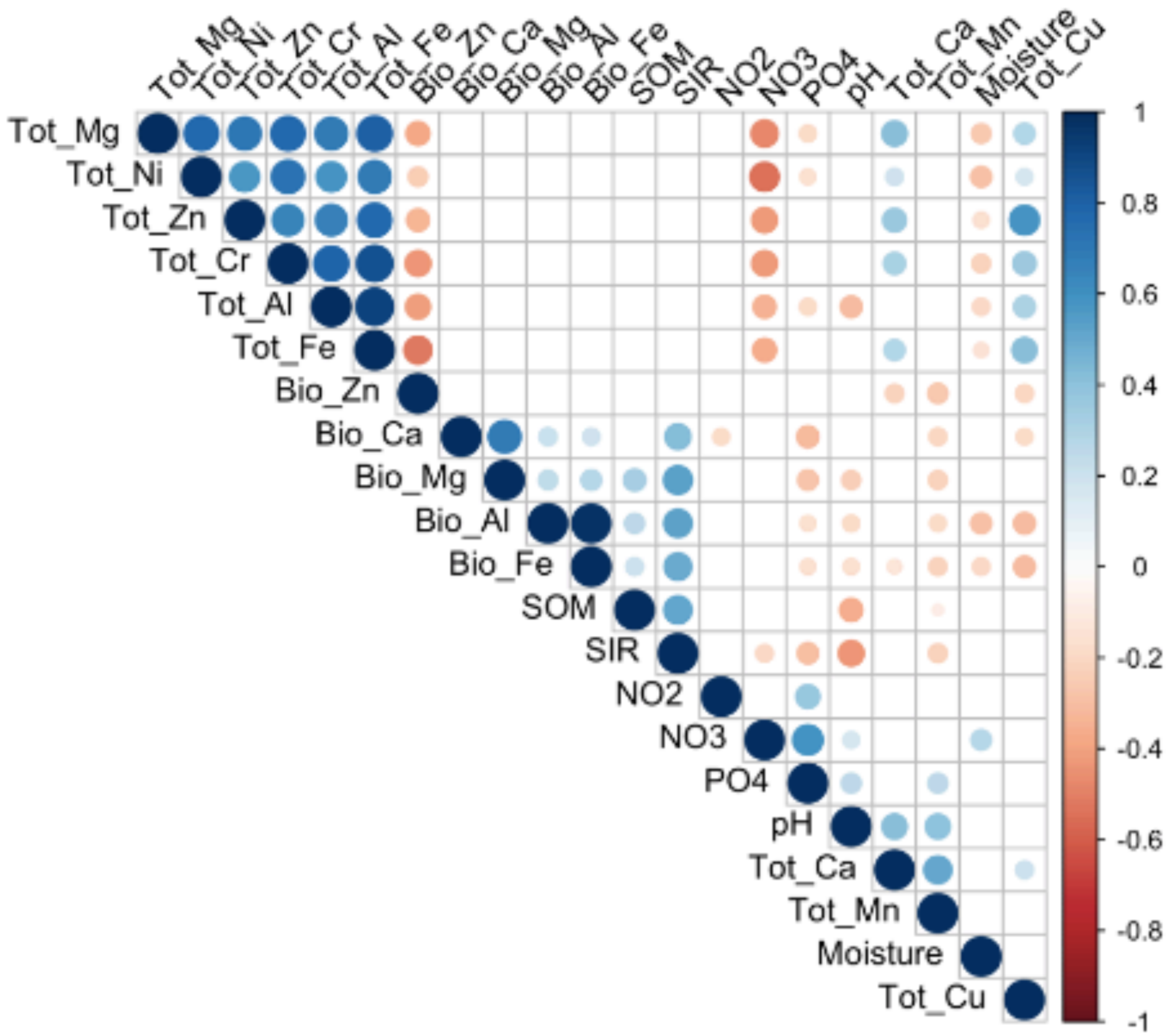

Fig. S5. Spearman correlations between the ranks of physicochemical characteristics and metal concentrations for sampled soils. Data includes soils basin bed and side slope samples for nine sampling locations (Fig. 2) of the study bioswales (BW1-4) (Fig. S1). The correlogram indicates significant correlations in blue (positive) and red (negative), where the size and color intensity of circles are proportional to the correlation coefficients. The legend (right) shows the coefficient values corresponding to the color scale. Blank spaces correspond to non-significant correlations ($\alpha = 0.05$). Total, and water soluble metals are indicated with the prefix “Tot”, and “Bio”, respectively.

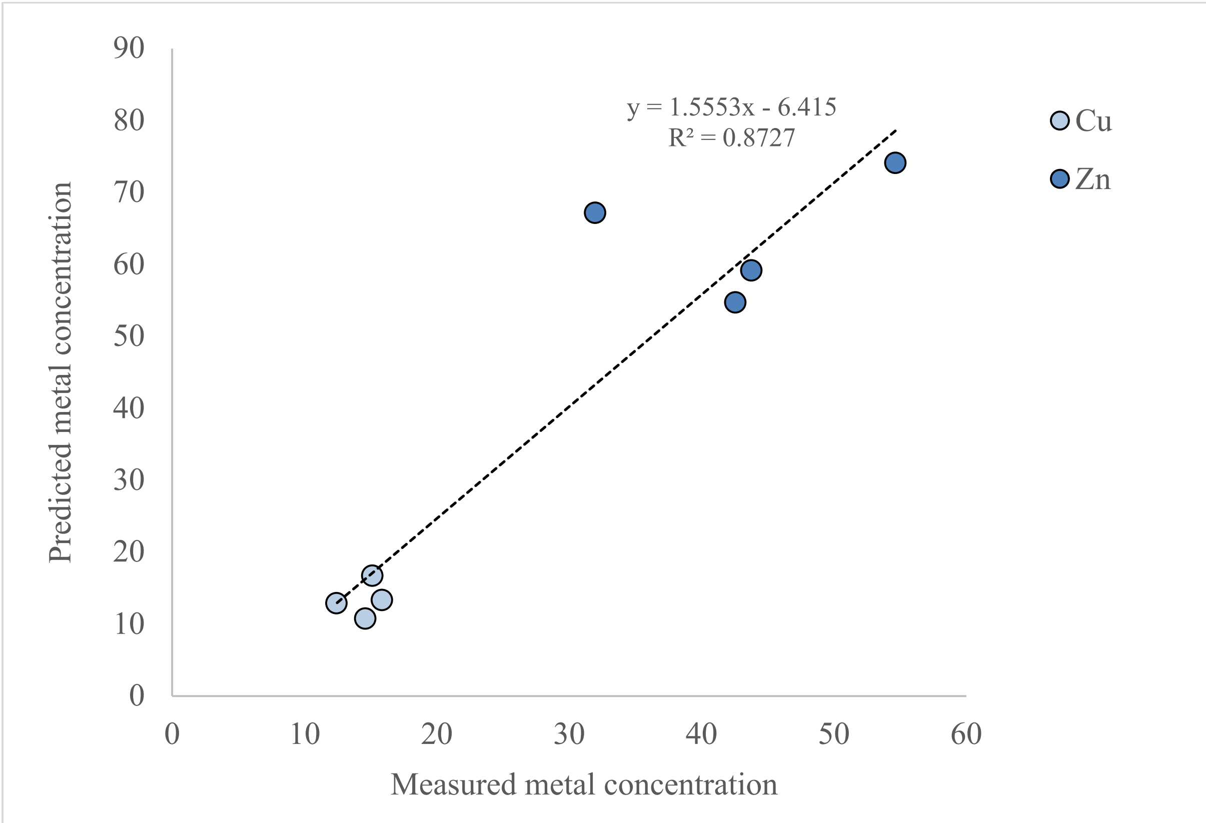

Fig. S6. Comparison between predicted and measured mean metal concentrations in sampled soils. Predicted metal concentrations were derived from the annual metal loads, years in operation, and background metal concentrations. Background metal concentrations were estimated as the first decile of all measured metal concentrations in sampled soils, including data from basin bed and side slope samples from nine sampling locations (Fig. 2) for study bioswales (BW1-4) (Fig. S1).

Table S1. Characteristics of tertiary treated and disinfected reclaimed water used for lawn irrigation in the study area. Data represents an annual average from monthly data from the Goleta Sanitary District 2017 Water Reclamation Annual Report (Goleta Sanitary 2018).

Parameter	**Value** [a]	**NPDES Limit** [b]
Turbidity, daily maximum (NTU)	1.90 (1.25)	5
Turbidity, daily average (NTU)	0.31 (0.13)	2
Total suspended solids (mg/L)	< 1.0 (0.1)	10
Biochemical oxygen demand (mg/L)	< 2 (0)	10
Settleable solids (mg/L)	< 0.1 (0.0)	0.1
pH (units)	7.0 (0.2)	6.5 - 8.4
Total coliform (MPN per 100 mL)	< 1.0 (0.0)	2.2
Chlorine residual minimum (mg/L)	15.4 (3.1)	5
Chlorine residual maximum (mg/L)	17.9 (1.8)	ns
Total dissolved solids (mg/L)	1,266 (111)	1500
Cadmium (μg/L)	0.31 (0.00)	0.01
Lead (μg/L)	2.96 (1.22)	5

[a] Values are mean and standard deviation (n = 12 for all parameters except total dissolved solids, n = 4, and cadmium and lead, n = 2).

[b] NPDES: National Pollutant Discharge Elimination System. Values represent water quality criteria in the NPDES permit for Goleta Sanitary District.

ns: not specified.

Table S2. Calculation parameters and results for yearly stormwater runoff entering study bioswales BW1-4. This calculation is derived from the average yearly precipitation and drainage area characteristics including directly connected impervious area, following the curve number method outlined in 210-VI-TR-55 (USDA 1986).

Parameter	BW1	BW2	BW3	BW4
Connected impervious area %	38	20	53	71
Pervious CN, open space > 75% cover, hydrologic soil group C[a]	74	74	74	74
Impervious CN[a], paved roads and roofs, hydrologic soil group C	98	98	98	98
Composite CN[b]	83	80	87	91
Potential maximum abstraction, S[c]	2.05	2.50	1.49	0.99
Average yearly runoff, Q (m)[d]	0.33	0.32	0.34	0.36
Average yearly runoff volume, V_R (m^3)[e]	1384	1290	553	789

[a] CN = curve number, obtained from Table 2-2a in 210-VI-TR-55 (USDA 1986)

[b] Composite curve number, obtained from Figure 2-3 in 210-VI-TR-55 (USDA 1986)

[c] S (in) = 1000/CN – 10 as per equation 2-4 in 210-VI-TR-55 (USDA 1986); S (mm) = S (in) x 25.4 mm/in

[d] Q given by equation 2-1 in 210-VI-TR-55 (USDA 1986), with I = initial abstraction = 0.05 following update suggested in Woodward et al. 2003 and converting from inches to meters.

[e] V_R = Q (m) x Drainage area (m^2) (Table 1).

Table S3. Total Cu concentrations in stormwater runoff entering low impact development (LID) sites in Santa Barbara, California. Runoff samples were collected by the City of Santa Barbara Creeks Division and tested for total recoverable metals by inductively coupled plasma-atomic emission spectroscopy (ICP-AES), following U.S. EPA method 6010B.

Station ID	Sample Type	Sample Date	Cu (mg/L)
LIDLot4	Grab	22/Jan/2009	0.049
LIDLot4	Grab	13/Oct/2009	0.090
LIDMacKen	Grab	07/Dec/2009	0.039
LIDMacKen	Grab	06/Oct/2010	0.013
LIDOakTenn	Grab	17/Nov/2012	0.010
LIDOakStag	Grab	17/Nov/2012	0.010
LIDStevePk	Grab	17/Nov/2012	0.011
LIDOakPicn	Grab	17/Nov/2012	0.016
LIDOakMain	Grab	17/Nov/2012	0.017
LIDWSNeigh	Grab	17/Nov/2012	0.031
LIDOakMain	Grab	24/Jan/2013	0.020
LIDOakPicn	Grab	24/Jan/2013	0.026
LIDOakTenn	Grab	24/Jan/2013	0.014
LIDWSNeigh	Grab	24/Jan/2013	0.026
LIDStevePk	Grab	24/Jan/2013	0.052
LIDOakMain	Composite	07/Mar/2013	0.012
LIDWSNeigh	Composite	07/Mar/2013	0.081
LIDOakTenn	Composite	07/Mar/2013	0.010
LIDStevePk	Composite	07/Mar/2013	0.011
LIDOakStag	Grab	24/Jan/2013	0.010
LIDOakPicn	Composite	07/Mar/2013	0.010
LIDOakStag	Composite	07/Mar/2013	0.010
Mean and standard deviation (mg/L)			0.026 (0.023)
Mean and standard deviation (mg/m^3)			25.8 (23.1)

Table S4. Total Zn concentrations in stormwater runoff entering low impact development (LID) sites in Santa Barbara, California. Runoff samples were collected by the City of Santa Barbara Creeks Division and tested for total recoverable metals via ICP-AES, following U.S. EPA method 6010B.

Station ID	**Sample Type**	**Sample Date**	**Zn (mg/L)**
LIDLot4	Grab	22/Jan/2009	0.240
LIDLot4	Grab	13/Oct/2009	0.120
LIDMacKen	Grab	07/Dec/2009	0.180
LIDMacKen	Grab	06/Oct/2010	0.084
LIDStevePk	Grab	17/Nov/2012	0.044
LIDOakPicn	Grab	17/Nov/2012	0.072
LIDOakStag	Grab	17/Nov/2012	0.082
LIDOakTenn	Grab	17/Nov/2012	0.095
LIDOakMain	Grab	17/Nov/2012	0.130
LIDWSNeigh	Grab	17/Nov/2012	0.290
LIDOakMain	Grab	24/Jan/2013	0.140
LIDOakPicn	Grab	24/Jan/2013	0.160
LIDOakStag	Grab	24/Jan/2013	0.042
LIDOakTenn	Grab	24/Jan/2013	0.084
LIDWSNeigh	Grab	24/Jan/2013	0.360
LIDStevePk	Grab	24/Jan/2013	0.310
LIDOakPicn	Composite	07/Mar/2013	0.057
LIDOakMain	Composite	07/Mar/2013	0.120
LIDOakStag	Composite	07/Mar/2013	0.027
LIDWSNeigh	Composite	07/Mar/2013	0.740
LIDOakTenn	Composite	07/Mar/2013	0.066
LIDStevePk	Composite	07/Mar/2013	0.053
Mean and standard deviation (mg/L).			0.159 (0.159)
Mean and standard deviation (mg/m^3)			159.(159)

References

Goleta Sanitary District (2018). 2017 Reclaimed Water Annual Report. Accessed on 08/23/20, available at https://goletasanitary.org/downloads/category/11-reclaimed-water

U.S. Department of Agriculture (1986). Urban hydrology for small watersheds. Technical Release 55, 210-VI-TR-55, Second Ed., Chapter 2, accessed on 07/04/2020, available at https://www.nrcs.usda.gov/Internet/FSE_DOCUMENTS/stelprdb1044171.pdf

Woodward, D., Hawkins, R., Jiang, R., Hjelmfelt, A., Mullem, J., and Quan, Q. (2003). Runoff curve number method: Examination of the initial abstraction ratio. World Water and Environmental Resources Congress. 1-10. 10.1061/40685(2003)308.